Memoirs of the Faculty of Engineering, Nagoya University
Vol. 29, No. 1. (1977)

ON THE PREDICTIVE, PRECOGNITIVE AND PREVIEW MANUAL TRACKING SYSTEMS

KOJI ITO and MASAMI ITO

Automatic control laboratory

(Received May 31, 1977)

CONTENTS

1. Introduction

Let's consider the problems of driving automobiles as an example of manual tracking behaviors. We can see ahead clearly in driving an automobile. This means that we can utilize the input (the roadway) in the future for the purpose of control at the present instant. If we cannot see ahead and know only the present position of the car, the satisfactory steering of the car will never be expected. In this case, we have to predict the future value from the present and past values of the input. Similar situation can be seen in the walk of man. We have to grope our way in the dark. But how about a familiar road? If we have remembered the input in the future from experience, it is possible to walk or drive smoothly to some extent without seeing ahead.

Thus, man obtains the information about the future value by predicting, or seeing the input function and utilizes skillfully it for the purpose of control at the present instant. This definitely depends on types of manual tracking systems. In this paper, therefore, manual tracking systems are grouped into three classes, i.e., predictive, precognitive and preview control systems;

(1) *Predictive control*: In a control system where no information is available to the operator except the present value of the input, the future value of the input must be predicted by the operator on the basis of the present and past input. This sort of control system is encountered when the operator is unable to grasp the features of the input because of inadequate training or because of random fluctuation of the input.

(2) *Precognitive control*[1]: If the input varies more or less regularly (consider, for example, a case where it varies nearly sinusoidally), the well-trained operator is able to store the future input in his memory as a result of repeated observation of the same input.

(3) *Preview control*[2]: in some cases, the operator is able to determine the future value of the input very definitely. Such a case occurs, for example, when a driver can see ahead clearly.

The purpose of this paper is to clarify the fundamental structures of the three classes of tracking control systems above from an angle of the control theory and then analyze experimentally the input tracking functions of the human operator.

We will here comment upon the fundamental principles and methods in developing mathematical and experimental analyses.

(1) In terms of idealizations, the simplest manual control system is considered as shown in the block diaglams of Fig. 1. 1. To control engineers, this configuration is a single input/ single output feedback system (apart from the feedbacks internal to the operator). Such a system is, itself, representative of many cases of practical interest and is, as well, a basic component of more complex multiloop system. For the system in Fig. 1. 1, there are four task variables which may have major effects on the operator's dynamics[3];

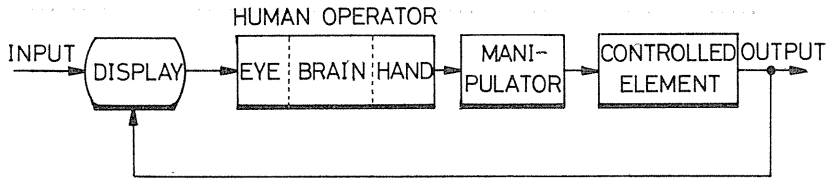

Fig. 1. 1. Simplified manual control system.

(i) *the input function characteristics* —— random appearing or periodic, continuous or discontinuous signal etc.,
(ii) *the controlled element dynamics* —— linear or nonlinear, stable or unstable, low order or high order controlled system etc.,
(iii) *the display* —— showing only the error (compensatory type), showing the input and output (pursuit type) or showing the future input and the present output (preview type) etc.,
(iv) *the manipulator* —— handle, stick etc..

Many other factors are implicitly involved. These include operator-centered variables such as training, fatigue, attention and motivation, and external environmental characteristics such as ambient illumination, humidity and temparature. In experiments performed to explore the effects of changes in the task variables upon the operator's dynamics, the operator-centered factors and the environmental characteristics are held constant.

(2) In this paper, the human operator is regarded as a black-box. On the basis of the facts which have been obtained in the field of physiology, it may be possible to divide the functions internal to the operator into the several blocks, i. e., the visual system, the cerebrum, the neuromuscular system etc.[4] But at the present stage it is yet impossible to represent the overall operator's response by means of synthesizing the characteristics of each block. Therefore, we don't refer to the physiological internal structure. We analyze the characteristics of the human operator from an angle of the contorl theory.

Modern research on the manual control of dynamic systems had it's origins in the work of *Tustin*[5] during the 1940's. Since then, most of the research in this field has been devoted to understanding the characteristics of the human as a controller of single variable, single display linear time-invariant systems such as one illustrated by the block diaglam of Fig. 1. 1.[6]~[15] With sufficient training in performing such a task, the human operator develops a relatively stable control

strategy and then is represented by the quasi-linear model, that is, as a describing function plus a remnant. The remnant is the portion of his output that cannot be related linearly to the input.[16]

The linear portion of the model consists of a transfer, or describing function and a set of rules for choosing its parameters. The complexity of the transfer function depends on the precision with which one attempts to reproduce the operator's characteristics. However, a fairly large body of data cad be acounted for by representative transfer function models in Tablel. 1. Each terms in Eq. (1-2) are as follows:

Table 1. 1. Typical transfer function models

Tustin[5]	$\frac{K(1+Ts)}{s}e^{-\tau s}$	(1-1)
McRuer & Krendel[3]	$\frac{K(1+T_L s)}{(1+T_I s)(1+T_N s)}e^{-\tau s}$	(1-2)
Iguchi[7]	$K\left(T_L s+1+\frac{1}{T_I s}\right)e^{-\tau s}$	(1-3)

$\frac{1}{1+T_N s}$; the neuromuscular dynamics is approximated linearly by an adjustable first-order lag. T_N is of the order $T_N=0.1$-0.6 sec with $T_N \cong 0.1$ being typical.

$e^{-\tau s}$; the human's pure time delay due to sensor excitation, nerve conduction, computation lags and other data processing activities in the central nervous system, where $\tau=0.1$-0.25 sec.

$\frac{K(1+T_L s)}{1+T_I s}$; the human's equlization characteristics which are adjustable according to the task requirements and are chosen such that the closed-loop characteristics will approximate those of a good feedback system.

The dependence of the human operator's characteristics on controlled element dynamics is fairly well explained by the crossover model proposed by *D.T. McRuer et al.*.[15] In Fig. 1. 2, let $G_P(s)$ be the transfer function of the operator and $G_c(s)$ be that for the contorlled element. Under the conditions that the input is random appearing signal, this model predicts that the operator adjusts parameters of $G_P(s)$

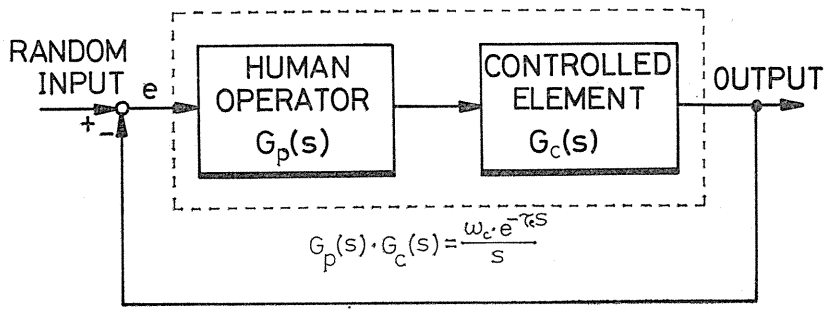

Fig. 1. 2. Crossover model.

depending on the controlled element dynamics and the input cut-off frequency such that

$$G_P(s)\cdot G_C(s)=\frac{\omega_c e^{-\tau_e s}}{s} \tag{1—4}$$

in the vicinity of angular frequency ω_c for which $G_P(s)\cdot G_C(s)=1$, where $\omega_c=3\sim5$ rad/sec, and $\tau_e=0.15\sim0.35$ sec. It has been reported that as the order of controlled element is increased, the operator tends to make ω_c smaller and τ_e larger.

The methods other than the transfer function models are based on the optimal control approach[17)~(20)] on the assumption that the human operator behaves "optimally" in some sense, and the sampled-data approach in which the human operator is regarded as a sampled-data system.[21)]

The quasi-linear models above are most useful for analyzing closed-loop compensatory tracking or state regulation tasks in which the human attempts to minimize some displayed system error, and form the foundation of analyzing more complex manual control systems. The compensatory tracking tasks are equivalent to predictive contool behavior in this paper since the inputs used are random-appearing signal. Therefore, the quasi-linear models are applicable to the predictive control system, but are not applicable to the others, i. e., precognitive and preview control systems.

Now, the "precognitive" control was named by *Krendel* and *McRuer*.[1)] They hypothesized a model for skill development based on "successive organization of perception" (SOP) in which it is assumed that the operator passes through all three topological phases in learning any tracking task. First, regardless of the display modality, the operator begins by concentrating on the error. As he recognizes certain characteristics of his response and becomes aware of the predictability of the input, he uses this information to behave as though he were in a pursuit tracking situation. Note that any input signal other than white noise will have some predictability even if it is not a periodic signal. Finally, when periodic or otherwise predictable inputs are recognized and learned, the subject begins to respond with well-practiced movements and is effectively tracking precognitively. *Pew et al.*[22)] examined experimentally the ability of a human to synchronize with single sine wave as an example of precognitive tracking.

No models useful for analyzing precognitive tracking are yet developed, however. In this paper, therefore, we propose the mathematical model to describe precognitive tracking tasks.

There is another type of tracking condition which is quite common, but which has received little attention. This is the case where the operator can see the future input as well as the present one. *T. B. Sheridon*[2)] has termed it "*preview control*" and also classified it into two categories; *forced-paced* and *self-paced*. The latter applies to the case where the operator is able to contorl his speed when traversing a corse, while the former applies to the case where the operator has no control over speed. The three models have been proposed by *Sheridon*.[2),(24)]

(1) *Extended convolution*; this model is an extension of simple linear convolution where the impulse response function extends into the future as well as into the past.

(2) *Fast time dynamic analog*; this presumes that the operator has an internal dynamic analog of himself and the controlled element, and is able to try a

control strategy and see how it works before beginning the real time strategy.

(3) *Iterative determination of optimal trajectory over the preview span*; this also incorporates a fast time dynamic analog like the second, but in addition, this has the ability to plan optimal trajectory over the preview time.

But he has not examined whether these models are applicable to the human operator in preview control systems. *Poulton*[23] did some experiments which pointed out the improvement in tracking accuracy when the subject had preview and/or postview. *Hayase et al.*[25] and *Tomizuka*[26] have theoretically proposed an optimal servo-system which utilizes the future value of the input. They are an extension of the conventional optimal tracking system.

As we have seen, no comparison has been made between these models and the experimental results in the preview manual control system. Therefore, we perform some experiments under various situations in forced-paced and self-paced preview control systems. By comparing the experimental results with our new preview models, we discuss how the operator processes the information abont the future input.

2. Structures of Predictive, Precognitive and Preview Control Systems[37]

2. 1. Introduction

Three fundamental tracking manual control systems, i. e., predictive, precognitive and preview control systems, are considered theoretically.

In section 2. 2, we define predictive and precognitive control systems on the basis of linear servo theory and, in section 2. 3, we define the preview control system on the basis of the optimal tracking theory. The relation between predictive and precognitive control systems is discussed in section 2. 4, and the relations between preview, predictive and precognitive control systems are discussed in section 2. 5.

2. 2. Linear servotheory and Predictive and Precognitive Control Systems

A control system is usually called a servosystem if the output signal is controlled so as to follow an reference input signal. In classical control theories, it has often been assumed that the reference signal does not vary randomly but varies stepwise or linearly with time.[28] Even in modern control theory based on the state space approach[29],[30], the reference input is assumed to be generated by a command generator, the response function of which is defined by

$$C.G.\begin{cases}\dot{z}=Gz & (2\text{—}1\,\mathrm{a})\\ r=h'z & (2\text{—}1\,\mathrm{b})\end{cases}$$

where G is (m×m)-constant matrix, h is (m×1)-constant vector and $(h'G)$ is observable. If, for instance,

$$G=\begin{pmatrix} 0 & 0 & 0 & \cdots & \cdots & 0 \\ 1 & 0 & 0 & 0 & \cdots & 0 \\ 0 & 1 & 0 & \cdots & \cdots & 0 \\ \cdots & \cdots & \cdots & \cdots & \cdots & \cdots \\ 0 & \cdots & \cdots & 1 & 0 & 0 \end{pmatrix}, \quad h=\begin{pmatrix} 0 \\ 0 \\ \vdots \\ 0 \\ 1 \end{pmatrix}, \tag{2—2}$$

and if the initial state of the command generator is given by

$$z'(0)=[z_{10},\ z_{20},\ \cdots,\ z_{m0}], \tag{2—3}$$

then the generated reference input $r(t)$ is expressed in terms of $(m-1)$th-order polynomial such that

$$r(t)=z_{m0}+z_{(m-1)0}t+\cdots+\frac{1}{(m-2)!}z_{20}t^{m-2}+\frac{1}{(m-1)!}z_{10}t^{m-1}, \tag{2—4}$$

On the other hand, if

$$G=\begin{pmatrix} 0 & \omega_1 & & & & \\ -\omega_1 & 0 & & & 0 & \\ & & 0 & \omega_2 & & \\ & & -\omega_2 & 0 & & \\ & 0 & & & 0 & \omega_r \\ & & & & -\omega_r & 0 \end{pmatrix}, \tag{2—5}$$

$$h=\begin{pmatrix} 1 \\ 0 \\ 1 \\ 0 \\ \vdots \\ 1 \\ 0 \end{pmatrix},$$

then the generated reference input is expressed in terms of a finite Fourier series such that

$$r(t)=\sum_{i=1}^{r} A_i\cos(\omega_i t+\varphi_i), \tag{2—6}$$

where A_i and φ_i are constants dependent upon intitial state $z(0)$.

As illustrated above, a considerably broad class of reference inputs can be generated by the command generator defined in Eq. (2-1).

When the reference input is restricted to the response function generated by

the command generator, the linear servoproblem in question is reduced to a regulator problem. Let's consider the controlled plant P defined by

$$\text{P.}\begin{cases}\dot{x}=Ax+bu & (2-7\,\text{a})\\ y=c'x, & (2-7\,\text{b})\end{cases}$$

where A is (n×n)-constant matrix, b and c are (n×1)-constant vectors, $(A,\ b)$ is controllable and $(c',\ A)$ is observable. If P is preceded by a dynamic compensator defined by

$$\text{D.C.}\begin{cases}\dot{u}=Bx+dv & (2-8\,\text{a})\\ u=u_1, & (2-8\,\text{b})\end{cases}$$

where

$$u=\begin{pmatrix}u_1\\ u_2\\ \vdots\\ u_p\end{pmatrix},\quad B=\begin{pmatrix}0 & 1 & 0 & \cdots & 0\\ 0 & 0 & 1 & \cdots & 0\\ \cdots & \cdots & \cdots & \cdots & \cdots\\ 0 & \cdots & \cdots & \cdots & 1\\ \alpha_1 & \alpha_2 & \cdots & \cdots & \alpha_p\end{pmatrix},\quad b=\begin{pmatrix}0\\ \vdots\\ 0\\ 1\end{pmatrix},\qquad (2-8\,\text{c})$$

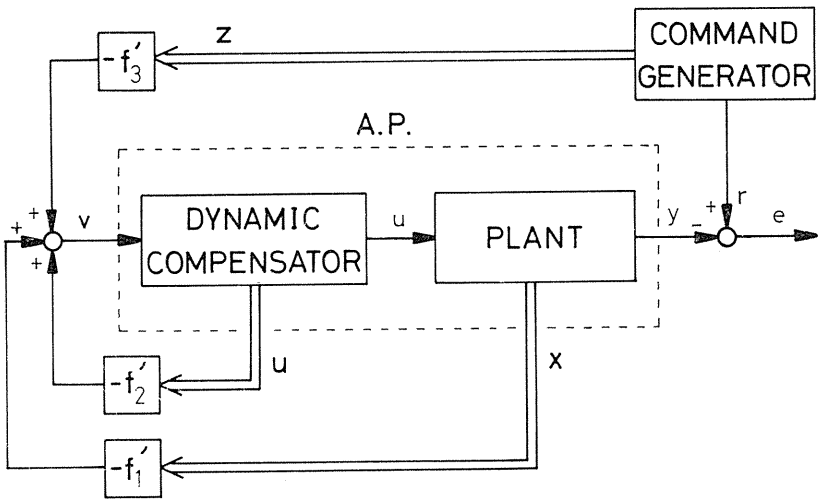

Fig. 2. 1. Servosystem with dynamic models.

then we call the combined system of plant (P) and dynamic compensator (D. C.) the augmented plant (abbreviated A. P.). It sbould be noticed here that A. P. is controllable if P is controllable. If A. P. is controllable and observable and if all the eigenvalues of command generator (G. C.) are involved in those of A. P., then the linear servoproblem can be reduced to a regulator problem.[29],[30] The steady-state error $(e=r-y)$ for $t\to\infty$ of this augumented plant (A. P.) vanishes independently

of initial states $x(0)$, $u(0)$ and $z(0)$ when states x, u and z are fed back as shown in Fig. 2. 1. Since it is impossible generally to measure z and x directly, it is necessary that they are estimated by means of some observer or via a suitable dynamic compensator.[31],[32] The servosystem thus constructed is shown in Fig. 2. 2.

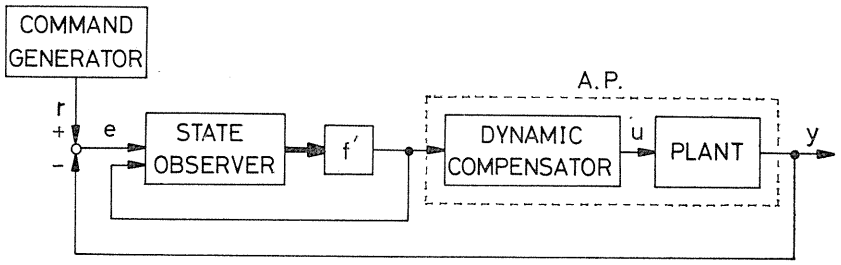

Fig. 2. 2. Servosystem with dynamic compensator and state observer.

Dynamic compensator (D. C.) must be designed so that eigenvalues of matrix $\begin{bmatrix} A & b0 \\ 0 & B \end{bmatrix}$ involve all those of matrix G. Accordingly, it becomes necessary to clarify the structure of command generator (C. G.) and to identify its parameters G and h in advance.[33] Since matrix B is designed after G and h have been identified, the control system under consideration is called *"a precognitive control system"*. Although the reference signal generated by the command generator depends not only on G and h but also on initial state $z(0)$, $z(0)$ can be chosen arbitrarily because the problem can be reduced to a regulator problem.

When reference input $r(t)$ is expressed in terms of a polynomial [see Eq. (2-4]], a dynamic compensator (D. C.) [see Eq. (2-8)] becomes integrators and state z of the command generator [see Eq. (2-1)] becomes $z'=[r^{(m-1)},\ldots, \ddot{r}, \dot{r}, r]$. This means that servosystem considered contains a differentiator, or if an observer[31] is used to estimate z from r, then it contains a pseudo-differentiator. While the servosystem following a polynomial input signal is nothing more than a well-known PID controller,[28] here we designate it *"a predictive control system"* because it contains a differentiator.

2. 3. Optimum Tracking Theory and Preview Control System

In section 2. 2, we have assumed that only the present value of the reference input is known. In this section, we assume that reference input $r(t)$ is known for $t_1 \leq t \leq t_2$ and attempt to determine the optimum control signal $u[x(t), t]$ which minimizes the performance function as defined by

$$J=\frac{1}{2}\Big\{[x(t_2)-r(t_2)]'M[x(t_2)-r(t_2)] + \int_{t_2}^{t_1}\{[x(t)-r(t)]'Q[x(t)-r(t)]+u^2(t)\}dt\Big\}, \qquad (2\text{—}9)$$

where M and Q are assumed not to vanish simultaneously. We also assume that reference input $r(t)$ is given by

$$r'(t)=[0,\ \cdots,\ 0,\ r(t)], \tag{2—10 a}$$

or

$$r'(t)=[r^{(n-1)}(t),\ \cdots,\ \ddot{r}(t),\ \dot{r}(t),\ r(t)], \tag{2—10 b}$$

and state equation (2-7) is represented by an observable canonical form[34] as follows:

$$A=\begin{pmatrix} 0 & 0 & 0 & \cdots & \cdots & -a_0 \\ 1 & 0 & 0 & \cdots & \cdots & -a_1 \\ 0 & 1 & 0 & \cdots & \cdots & -a_2 \\ \cdots & \cdots & \cdots & \cdots & \cdots & \cdots \\ 0 & \cdots & \cdots & \cdots & 1 & -a_{n-1} \end{pmatrix},\quad b=\begin{pmatrix} b_0 \\ b_1 \\ \vdots \\ \vdots \\ b_{n-1} \end{pmatrix},\quad c=\begin{pmatrix} 0 \\ 0 \\ \vdots \\ 0 \\ 1 \end{pmatrix}. \tag{2—11}$$

The above problem is usually called an optimum tracking problem and its solution is given in (35), according to which the optimal solution is given by

$$u(t)=b'[g(t_2-t)-K(t_2-t)x(t)]. \tag{2—12}$$

In Eq. (2-12), $g(t_2-t)$ and $K(t_2-t)$ are the solutions for the following differential equations:

$$\begin{cases} \dot{K}(t_2-t)=K(t_2-t)bb'K(t_2-t)-K(t_2-t)A \\ \qquad -A'K(t_2-t)-Q & (2—13\,a) \\ K(t_2-t)|_{t=t_2}=M, & (2—13\,b) \end{cases}$$

$$\begin{cases} \dot{g}(t_2-t)=[K(t_2-t)bb'-A']g(t_2-t)-Qr(t), & (2—14\,a) \\ g(t_2-t)|_{t=t_2}=Mr(t_2). & (2—14\,b) \end{cases}$$

Substituting Eq. (2-12) into Eq. (2-7), we obtain the following equation for a closed-loop system:

$$\begin{cases} \dot{x}=[A-bb'K(t_2-t)]x+bb'g(t_2-t), & (2—15\,a) \\ y=c'x. & (2—15\,b) \end{cases}$$

It should be noticed here that $g(t_2-t)$ and $K(t_2-t)$ are known in advance for $t_1\leq t\leq t_2$. In particular, $g(t_2-t)$ is determined from Eq. (2-14a) using $r(t)$ known for $t_1\leq t\leq t_2$. Since the optimal tracking system tracks a known reference input, it is essentially different from a servosystem which pursues an unknown reference input. In this sense, the optimal tracking system is a programmed control system. Consequently, if the reference input deviates from a presumed value, the tracking system is unable to operate optimally.

Hayase et al.,[25] to improve this fact, proposed a control system which has the following properties.

(1) Reference input $r(t)$ for the entire time range $t\in[t_1,\ t_2]$ is not known a

priori while it is always possible to measure the reference input $r(\tau)$ for a certain future time period $\tau \in [t,\ t+t_f]$ at arbitrary time t.

(2) Set up the optimal tracking system for $\tau \in [t,\ t+t_f]$, for which Eqs. (2-12) to (2-14) are rewritten as

$$u(\tau)=b'[g(t+t_f-\tau)-K(t+t_f-\tau)x(\tau)], \tag{2—16}$$

$$\begin{cases} \dot{K}(t+t_f-\tau)=K(t+t_f-\tau)bb'K(t+t_f-\tau) \\ \quad -K(t+t_f-\tau)A-A'K(t+t_f-\tau)-Q, & (2—17\,a) \\ K(t+t_f-\tau)|_{\tau=t+t_f}=M, & (2—17\,b) \end{cases}$$

$$\begin{cases} \dot{g}(t+t_f-\tau)=[K(t+t_f-\tau)bb'-A']g(t+t_f-\tau)-Qr(t) & (2—18\,a) \\ g(t+t_f-\tau)|_{\tau=t+t_f}=Mr(t+t_f). & (2—18\,b) \end{cases}$$

Solving Eqs. (2-17) and (2-18) backward with respect to time, we can determine the value of K and g for $\tau=t$. Accordingly, control signal $u(t)$ is given by

$$u(t)=b'[g(t_f)-K(t_f)x(t)], \tag{2—19}$$

where $K(t_f)$ is a constant independent of time t. Since $r(\tau)$ varies with time t, it is necessary to recalculate the value of g for $\tau \in [t,\ t+t_f]$ using Eq. (2-18) whenever t varies.

(3) The tracking system mentioned in the above item can be realized by a servosystem equipped with a high-speed computer which calculates the value of $g(t)$ using Eq. (2-18) [see Fig. 2. 3]. In (25), the integration in Eq. (2-18) is performed by summation.

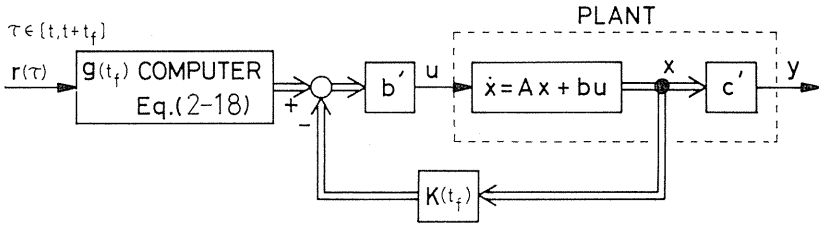

Fig. 2. 3. Servosystem utilizing the future value of input function (preview control system).

In the above discussion, the value of the reference input for a certain time period in the future is assumed to be known, and here we call this "*a preview control system*". It may be estimated here that the longer t_f is, the better the control performance becomes. According to (25), however, the control performance is not improved greatly even if t_f is too large. In practice, it is sufficient for t_f to be slightly larger than the peak time of the impulse response of the closed-loop system in Fig. 2. 3.

2. 4. Relation between Predictive and Precognitive Control Systems

In this section, we discuss the relation between predictive and precognitive control systems and show that the two systems have almost the same control performance if the control signal energy is not limited.

Since command generator (C. G.) defined by Ep. (2-1) is observable, G is a nonderogatory matrix.* Further, expressing Eq. (2-1) in Jordan form, we can express G and h[34),(37)]

$$G=\begin{pmatrix} \lambda_1 & 1 & 0 & & & & \\ & \ddots & \ddots & & & & \\ & & \lambda_1 & & & & \\ & & & \lambda_2 & 1 & 0 & \\ & & & & \ddots & \ddots & \\ & & & & & \lambda_2 & \\ & & & & & & \ddots \\ & & & & & & \lambda_l \end{pmatrix}, \qquad h=\begin{pmatrix} h_{11} \\ \vdots \\ h_{1q_1} \\ h_{21} \\ \vdots \\ h_{2q_2} \\ \vdots \\ h_{l_1} \\ \vdots \\ h_{lq_l} \end{pmatrix}, \tag{2—20 a}$$

where

$$\left.\begin{aligned} &\lambda_1 \fallingdotseq \lambda_2 \fallingdotseq \cdots\cdots \fallingdotseq \lambda_l \\ &m=q_1+q_2+\cdots+q_l \\ &h_{11},\ h_{21},\ \cdots,\ h_{l_1} \fallingdotseq 0 \end{aligned}\right\}. \tag{2—20 b}$$

*) If there exists only one independent eigenvector for each different eigenvalue λ_1, $\lambda_2 \cdots \lambda_s$ $(s \leq n)$ of n×n matrix A, then A is called a nonderogatory matrix (36).

Consequently, output $r(t)$ of command generator (C. G.) is expressed as

$$r(t)=h'\exp(Gt)z(0)$$
$$=\sum_{i=1}^{r} f_i(t)e^{\lambda_i t}+\sum_{j=1}^{s} f_j(t)e^{a_j t}\times\cos(b_j t+\varphi_j), \qquad (2\text{—}21)$$

where $r+2s=l$ and $\lambda_j=a_j+jb_j$. If G and h are given by Eq. (2-2), $l=1$, $q_1=m$, $\lambda_1=0$ and $h_{11}=1$. In Eq. (2-21), $f_i(t)$ and $f_j(t)$ are (q_i-1) th- and (q_j-1) th-order polynomials, respectively, the coefficients of which are dependent upon $h_{11}\cdots h_{\ell q_\ell}$ and initial state $z(0)$. Approximating $e^{\lambda_j t}$ and $e^{a_j t}\cos(b_j t+\varphi_j)$ in terms of $(m-q_i)$ th- and $(m-q_j)$ th-order polynomials, respectively, we can express $r(t)$ in terms of an $(m-1)$st-order polynomial, the coefficients of which are dependent upon h, $z(0)$ and λ_i (i=1, 2, ···, l). Consequently, $r(t)$ thus expessed is of the same form as that in Eq. (2-4). This means that the predictive control designed for the polynomial reference input is able to respond to an arbitrary reference input satisfying Eq. (2-1). Further, the performance of this control system is dependent upon the approximation accuracy of $e^{\lambda_j t}$ and $e^{a_j t}\cos(b_j t+\varphi_j)$ as described below.

(i) The larger m is or, equivalently, the higher the approximation accuracy, the more the predictive control system behaves like the precognitive control system. However, when m is larger, the controller (dynamic compensator [see Eq. (2-8)] plus observer) has a complicated structure and becomes expensive.

(ii) If $|\lambda_i t|$, $|a_j t|$ and $|b_j t|$ are small, or, equivalently, if t is small, the approximation accuracy is high. This means that when the closed-loop system has a sufficiently high-speed response time, the predictive control system has almost the same response performance as the precognitive control system although the amplitude of the control signal necessarily becomes large.[28]

As an illustrative example, the response curve of a predictive control system is compared with that of a precognitive control system as shown in Fig. 2. 4, where

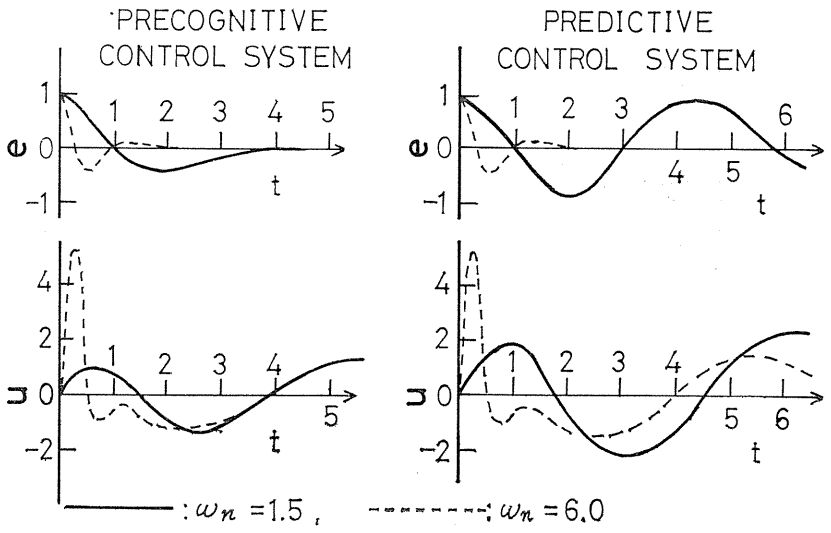

Fig. 2. 4. Responses of precognitive and predictive control system with a sine wave input (first-order plant).

the reference input is assumed to be

$$r(t)=\cos \omega_0 t \tag{2—22}$$

and the behavior of the controlled plant is described by

$$\left.\begin{aligned}\dot{x}&=-\alpha\dot{x}+u\\ y&=x.\end{aligned}\right\}. \tag{2—23}$$

The predictive and the precognitive cotrol systems are constructed through the procedures described in section 2. 2. Reference input $r(t)$ given by Eq. (2-22) is approximated to a first-order polynomial for the predictive control system and parameters of both the predictive and the precognitive control systems are designated so that the characteristic polynomial for the closed loop is expressed in terms of Butterworth one $(s^2+2\omega_n s^2+2\omega_n{}^2 s+\omega_n{}^3)$.

In Fig. 2. 4, ω_n is set equal to 1.5 and 6 ($\omega_0=1$ and $\alpha=1$). When $\omega_n=6\omega_0$, even the predictive control system is able to follow the sinusoidally varying reference input very satisfactorily while the amplitude of the control signal inevitably becomes large. By contrast, when $\omega_n=1.5\omega_0$, the predictive control system is not able to respond as quickly as the precognitive control system. The response of the predictive control system can be improved by using a higher-order controller as stated in item (i) of section 2. 4. To summarize the above discussion, the relation between predictive and precognitive control systems is affected greatly by: (i) the energy of the control signal, (ii) the order of the controller, and (iii) the identification accuracy of the reference input.

2. 5. Relation between Predictive, Precognitive and Preview Control Systems

In this section we discuss the relation between the three fundamental control systems, and show that when the preview time is sufficiently large, the preview control system has the same structure as the predictive or the precognitive control system.

An automobile operator is unable to drive a car safely unless he can see ahead clearly. This is true even if he passes the same road every day. Theoretically speaking, however, it is possible for him to drive safely without looking ahead if he memorizes all the features of the road very accurately and if he is aware of where he is. In fact, a well-trained operator is able to follow the reference input varying in a simple fashion even if he knows only the present value of the reference input.[1],[22] By contrast, when the reference input varies in a complicated way, the operator may not be able to identify it accurately or have the dynamic model of sufficient accuracy to reproduce it within himself.

On the other hand, a purely mechanical control system which does not contain manual operators may be afforded a sufficiently accurate response performance. Therefore if the given reference input belongs to a class defined by Eq. (2-1), it will be possible to let the predictive or the precognitive control system equipped with a dynamic compensator have almost the same performance as the preview control system defined in section 2. 3.

To study the above statement theoretically, let us consider a peredictive or

precognitive control system for an augmented plant (A. P.) defined by

$$\begin{cases} \dot{w}=\bar{A}w+\bar{d}u_c \\ y=\bar{c}'w, \end{cases} \tag{2—24}$$

where

$$w=\begin{bmatrix} x \\ u \end{bmatrix}, \quad \bar{A}=\begin{bmatrix} A & b0 \\ 0 & B \end{bmatrix}, \quad \bar{c}=\begin{bmatrix} c \\ 0 \end{bmatrix}, \quad \bar{d}=\begin{pmatrix} 0 \\ \vdots \\ 0 \\ 1 \end{pmatrix}.$$

If the augmented plant defined by Eq. (2-24) is observable and controllable, and if the eigenvalues of this plant contains all those of Eq. (2-1), then we can reduce the steady-state error to zero by applying the control signal such that

$$\begin{aligned} u_c(t) &= -f_1'x-f_2'u-f_3'z \\ &= -k'w-f_3'z, \end{aligned} \tag{2—25}$$

where K' is an $(n+p)$ vector equal to $[k_1, \cdots, k_{n+p}]$. Further, according to Eq. (2-1),

$$z=\exp(Gt)z(0), \tag{2—26}$$

which we substitute into Eq. (2-25) to obtain

$$u_c(t)=-\sum_{i=1}^{l} g_i(t)e^{\lambda_i t}-\sum_{i=1}^{n+p} k_i w_i(t), \tag{2—27}$$

where λ_i is usually a complex-valued eigenvalue and $g_i(t)$ is the (q_i-1)th-order polynomial.

On the other hand, control signal $u(t)$ for the preview control system is given by Eq. (2-19) [see Fig. 2. 3.], where $K(t_f)$ specifies the transient response of the closed-loop system in Fig. 2. 3 and can be derived from Eq. (2-17). However, Eq. (2-17) is independent of reference input $r(t)$ and, consequently, it is not admissible for $K(t_f)$ to vary with t_f. This means that $K(t_f)$ is independent of t_f and is constant. In order for $K(t_f)$ to be independent of t_f, final value M of Eq. (2-17) for $\tau=t+t_f$ must be a stable steady-state solution for Eq. (2-17a). Since feedback gain $K(t_f)$ is constant, forward gain $g(t_f)$ can be calculated very easily by measuring only the future value of the reference input. Function $g(t_f)$ is determined by solving a differential equation (2-18) with time-invariant coefficients. That is, for $\tau=t$,

$$g(t_f)=\exp[-Wt_f]Mr(t+t_f)+\int_t^{t+t_f}\exp[W(t-\tau)]Qr(\tau)d\tau, \tag{2—28}$$

where

$$W=[K(t_f)bb'-A']. \tag{2—29}$$

The preview control system described above is shown in Fig. 2. 5.

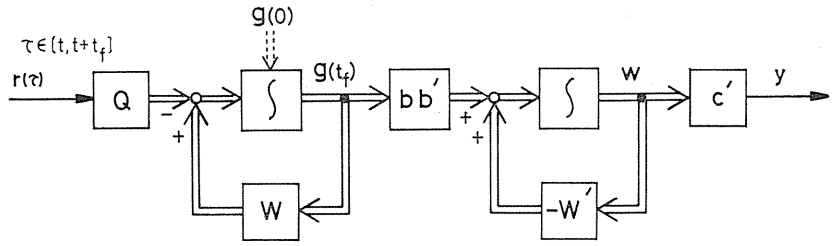

Fig. 2. 5. Preview control system.

Rewriting W in Jordan standard from, we obtain

$$\exp(Wt)=\exp(PJP^{-1}t)=P\exp(Jt)P^{-1}, \qquad (2\text{—}30\,a)$$

where P is a regular matrix. Further, since W is a nonderogatory matrix, J is expressed as

$$J=\begin{pmatrix} \begin{matrix}\bar{\lambda}_1 & 1 & & 0\\ & \ddots & \ddots & \\ & & \ddots & 1\\ 0 & & & \bar{\lambda}_1\end{matrix} & & & \\ & \begin{matrix}\bar{\lambda}_2 & 1 & & 0\\ & \ddots & \ddots & \\ & & \ddots & 1\\ 0 & & & \bar{\lambda}_2\end{matrix} & & \\ & & \ddots & \\ & & & \begin{matrix}\bar{\lambda}_s & 1 & & 0\\ & \ddots & \ddots & \\ & & \ddots & 1\\ 0 & & & \bar{\lambda}_s\end{matrix}\end{pmatrix}, \qquad (2\text{—}30\,b)$$

where

$$\sum_{j=1}^{s}\gamma_j=n,\quad \bar{\lambda}\neq\cdots\cdots\neq\bar{\lambda}_s.$$

Setting

$$u_1(t)=b'g(t_f), \qquad (2\text{—}31)$$

we obtain the following equation from Eq. (2-28) :

$$u_1(t)=b'\left[Pe^{-Jt_f}P^{-1}Mr(t+t_f)+\int_t^{t+t_f}Pe^{J(t-\tau)}P^{-1}Qr(\tau)d\tau\right]. \qquad (2\text{—}32)$$

On the other hand, Eqs. (2-20) and (2-21) give

$$r(t)=\sum_{i=1}^{l}\varphi_{q_i}(t)\,e^{\lambda_i t}, \tag{2—33}$$

where λ_i is a complex-valued eigenvalue and φ_{q_i} is a (q_i-1)st-order polynomial. Substituting Eq. (2-33) into Eq. (2-32) and using Eq. (2-10a), we obtain

$$u_1(t)=\sum_{i=1}^{l}\sum_{j=1}^{s}[f_{ij}(t,\ t_f)e^{\lambda_i t}e^{(\lambda_i-\bar{\lambda}_j)t_f}-f_{ij}(t)e^{\lambda_i t}], \tag{2—34}$$

where f_{ij} is the $(q_i+\gamma_j-2)$nd-order polynomial and $R_e\{\lambda_i\}$ is assumed to be less than $R_e\{\bar{\lambda}_i\}$ for all values of i and j. (Since $\bar{\lambda}_j$ is an eigenvalue of the adjoint system, its real part is positive and therefore the above assumption is not so severe.) Letting t_f be sufficiently large

$$\begin{aligned}u_1(t)&\simeq-\sum_{i=1}^{l}\sum_{j=1}^{s}f_{ij}(t)e^{\lambda_i t}\\&=-\sum_{i=1}^{l}\bar{f}_i(t)e^{\lambda_i t},\end{aligned} \tag{2—35}$$

which we substitute into Eq. (2-19) to get

$$u(t)=-\sum_{i=1}^{l}\bar{f}_i(t)e^{\lambda_i t}-\sum_{j=1}^{n}\bar{k}_j x_i(t). \tag{2—36}$$

Comparing Eq. (2-36) with Eq. (2-27), we see that the preview control system has the same structure as the predictive or the precognitive control system when t_f is sufficiently large.

To confirm the validity of the above statement, let us consider again the example in section 2. 4. When the reference input and the controlled plant are given by Eqs. (2-22) and (2-23), respectively, Eqs. (2-17) to (2-19) can be rewritten respectively as

$$\dot{K}(t+t_f-\tau)=K^2(t+t_f-\tau)+2\alpha K(t+t_f-\tau)-q, \tag{2—37}$$

$$K(t+t_f-\tau)|_{\tau=t+t_f}=m,$$

$$\dot{g}(t+t_f-\tau)=[K(t+t_f-\tau)+\alpha]g(t+t_f-\tau)-q\cdot\cos\omega_0\tau, \tag{2—38}$$

$$g(t+t_f-\tau)|_{\tau=t+t_f}=m\cdot\cos\omega_0(t+t_f),$$

$$u(t)=g(t_f)-K(t_f)x(t). \tag{2—39}$$

Letting backward initial value m be a stable steady-state solution for Eq. (2-37), we obtain

$$m=K(t+t_f-\tau)|_{\tau=t}=K(t_f)=-\alpha+\sqrt{\alpha^2+q}. \tag{2—40}$$

Therefore,

$$g(t_f)=e^{-\{K(t_f)+\alpha\}t_f}\cdot m\cdot\cos\omega_0(t+t_f)$$
$$+\int_t^{t+t_f}e^{\{(K(t_f)+\alpha\}(t-\tau)}\cdot q\cdot\cos\omega_0\tau d\tau$$
$$=e^{-\{K(t_f)+\alpha\}t_f}\left[\left(K(t_f)-\frac{q\{K(t_f)+\alpha\}^2}{{\omega_0}^2+\{K(t_f)+\alpha\}^2}\right)\cos\omega_0(t+t_f)\right.$$
$$\left.+\frac{q\omega_0}{{\omega_0}^2+\{K(t_f)+\alpha\}^2}\sin\omega_0(t+t_f)\right]$$
$$+\frac{q}{{\omega_0}^2+\{K(t_f)+\alpha\}^2}[\{K(t_f)+\alpha\}\cos\omega_0 t-\omega_0\sin\omega_0 t]. \quad (2-41)$$

Notcing that $K(t_f)+\alpha>0$ and letting t_f be sufficiently large, we obtain

$$g(t_f)\cong\frac{q}{{\omega_0}^2+\{K(t_f)+\alpha\}^2}[\{K(t_f)+\alpha\}\cos\omega_0 t-\omega_0\sin\omega_0 t]. \quad (2-42)$$

Since

$$r(t)=\cos\omega_0 t$$

and

$$\dot{r}(t)=-\omega_0\sin\omega_0 t,$$

we obtain

$$u(t)=f_{p_1}r(t)+f_{p_2}\dot{r}(t)-K(t_f)x(t), \quad (2-43)$$

where

$$f_{p_1}=\frac{q\{K(t_f)+\alpha\}}{{\omega_0}^2+\{K(t_f)+\alpha\}^2}$$

$$f_{p_2}=\frac{q}{{\omega_0}^2+\{K(t_f)+\alpha\}^2}.$$

Consequently, the forward path has the same structure as the predictive or the precognitive control system. While the preview control system contains no dynamic compensator in its feedback loop, it is possible to let it behave almost in the same way as the predictive or the precognitive control system, because the transient response of the closed-loop system can be adjusted freely by regulating the feedback gain. In Fig. 2. 6, we have set $q=1.25$ and $t_f=1.0$ (chain curves), $q=35$ and $t_f=0.0$ (dotted curves) and $q=35$ and $t_f=1.0$ (solid curves): $q=1.25$ and $q=35$ correspond to $\omega_n=1.5$ and $\omega_n=6$ ($\omega_0=1$ and $\alpha=1$) respectively. As illustrated in Fig. 2. 6, the response performance is not good unless the loop gain is high. This means that a control signal must have a large amplitude. Note here that the control performance can not be improved by letting t_f be larger. Following the three statements mentioned in section 2. 4, we can draw the following conclusions:

(i) the control signal becomes larger inevitably,

(ii) if $g(t_f)$ is regarded as a controller, its order depends on the structure of a controlled system,

(iii) utilization of the future value of the reference input signifies the reference input being identified.

As stated above, the preview control system has the same structure and the same response performance as the predictive or the precognitive contorl system when the preview time is sufficiently large. However, when the reference input can not be described in terms of a differential equation with time-invariant coefficients (see, for instance, an unpredictable reference input as shown in Fig. 2. 7), the preview control system is clearly superior to the predictive or the precognitive control system. In this sense, the preview control system responds very effectively to an unpredictable reference signal.

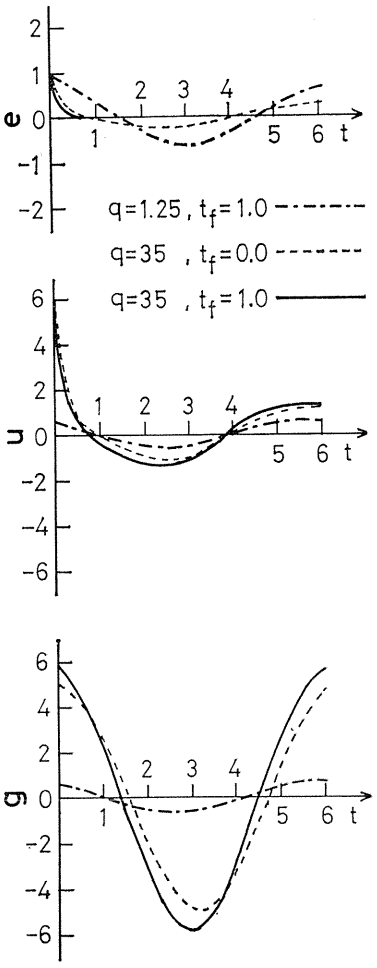

Fig. 2. 6. Responses of preview control system with a sine wave input (first-order plant).

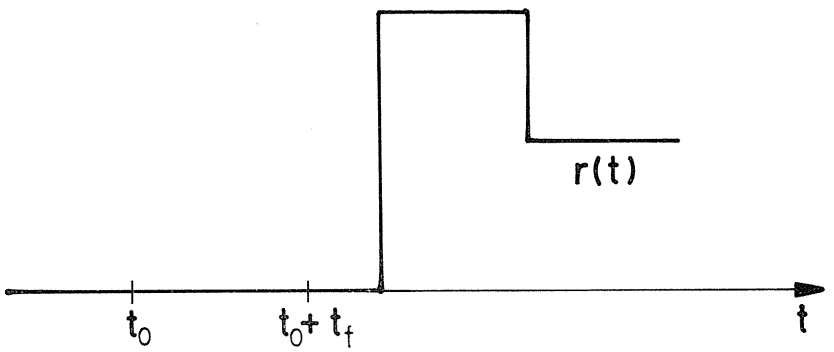

Fig. 2. 7. An example of unpredictable input.

2. 6. Summary

(1) If the reference input is generated by time-invariant linear system, and if no restriction is imposed upon the magnitude of the control signal, then the servo-system based on classical control theory exhibits a satisfactory response. This servosystem is a kind of predictive control system and neither a precognitive nor a preview control system of complicated structure has to be used.

(2) The precognitive control system is superior to the predictive control system if the reference input can be identified relatively easily and if a lower-order dynamic compensator can be used.

(3) The preview control system is superior to the predictive or the precognitive control system if the reference input is not predictable.

Thus, we analyzed theoretically the functions of the three fundamental control systems, i. e., predictive, precognitive and preview ocntrol systems. On and after the next chapter, we discuss some experimental results of the manual tracking behaviors and analyze the fundamental structures of them from an angle of the three control systems above.

3. Predictive and Precognitive Manual Tracking,[38]

3. 1. Introduction

The simplest form of the input adaptation is the ability of the human operator to recognize periodic input signal or even periodic components in the input signal and use the predictive nature of these signals to synchronize his response. For example, if the input varies regularly as an example of single single sine wave, the operator has effectively complete information about the input's future and so it is tracked in a precognitive mode.[1] If the input coherence is poor, however, the operator has only limited information about the input's future and he always attempts to do some prediction on the input signal.

The purpose of this chapter is to experimentally analyze the predictive and precognitive tracking behaviors of the human opertor and answer the question; "*how does the operator vary his effective control topology with input signal coherence?*" A means for approaching this problem is to start with a sine wave and to add successively more and more sinusoids of given frequencies, amplitudes and phases.[39] In this case, the repetitiveness of the input may be reduced gradually.

In this chapter, we experimentally investigate how the tracking behaviors of the human operator varies from precognitive control to predictive control when he tracks three kinds of the inputs; single sine wave, 2 sine waves and 3 sine waves.

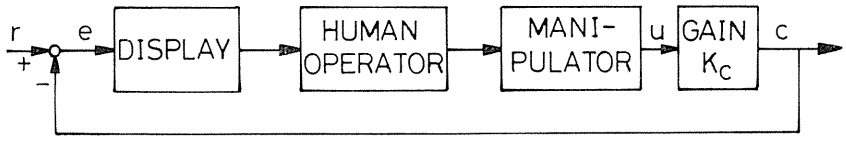

Fig. 3. 1. Compensatory manual control system.

3. 2. Experiments

3. 2. 1. Experimental arrangement

As shown in Fig. 3. 1, the experiments were performed in compensatory manual control systems in which only the error signal was shown to the subject. The visual display was an osilloscope 14 cm in diameter on which the spot moved horizontally. The peak amplitude of spot motion was 4 cm. The manipulator was a round handle 5 cm in diameter which had negligible damping and inertia, and 45 deg. on the round handle corresponded to 4 cm on the oscilloscope. A pure gain controlled element was used so that the human operator was able to easily learn the characteristics of the input signal. Seven male subjects from 22 to 27 years old were employed in the experiments.

The experiments were performed for three kinds of the input signals; single sine wave, 2 sine waves and 3 sine waves. These sine waves were composed of all different frequencies, same amplitudes and random phases. For each such input, three subjects were asked to perform the trials. But the experimental results which are shown in Tables 3. 1 ~ 3. 3 are the average values of 10 trials of the operator with the best scores.

3. 2. 2. Experimental procedure

The operator was instructed to minimize the error displayed on an osciloscope as the horizontal distance of a spot from the center and each trial run was performed for 60 sec. The operator's eyes were about 50 cm from the scope.

The mean square value S_e was computed for each trial.

$$S_e=\int_0^{60} e(t)^2dt/\int_0^{60} r(t)^2dt, \tag{3—1}$$

where $r(t)$ denotes the input signal and $e(t)$ denotes the tracking error. Then, each operator was trained until S_e reached a constant level from run to run. After the operator was well-trained, 10 trial runs of 60 sec duration were carried out and the following were computed:

(1) The mean square value S_e.
(2) The power spectral $\Phi_e(jf)$ of the error signal.
(3) The input-output amplitude ratio $g(f_i)=|C(jf_i)|/|R(jf_i)|$.
(4) The input-output phase difference $\varphi(f_i)=\angle C(jf_i)-\angle R(jf_i)$, where $R(jf_i)$ and $C(jf_i)$ are the Fourier transform of the input signal $r(t)$ and the output $c(t)$ of the operator, and f_i is input frequency and is shown Table 3. 1~3. 3.
(5) The time $\tau(f_i)$ which is equivalent to the phase difference $\varphi(f_i)$ at each frequency f_i.

$$\tau(f_i)=\varphi(f_i)\times\frac{1}{360}\times\frac{1}{f_i}\text{sec.} \tag{3—2}$$

3. 3. Experimental results

3. 3. 1. Single sine wave tracking

Table 3. 1 presents input-output amplitude ratios and phase differences, and mean square values S_e of the errors measured from the experiments, where the

Table 3. 1. Single sine wave tracking (averaged over 10 trials).

Input frequency (f_i) Hz	0.1	0.2	0.4	0.6	1.0	1.2
Input-output amplitude ratio (g)	1.0	1.0	0.99	0.98	0.93	0.91
Input-output phase difference (φ) and standard deviation	−1.0° ±0.3	−0.8° ±0.3	0.0° ±1.1	−0.6° ±1.1	−1.5° ±3.6	−1.0° ±7.4
Mean square value (Se)	0.03	0.07	0.1	0.1	0.18	0.27

inputs were single sine waves of six kinds of the frequencies between 0.1 Hz and 1.2 Hz, and every data is averaged over 10 trials.

At every input frequency, the input-output amplitude ratios are almost unity and the phase differences are negligible small. That is, single sine wave is relatively easy to recognize the input coherence. The operator does not need to follow the input a reaction time behind and is able to synchronize almost perfectly with the

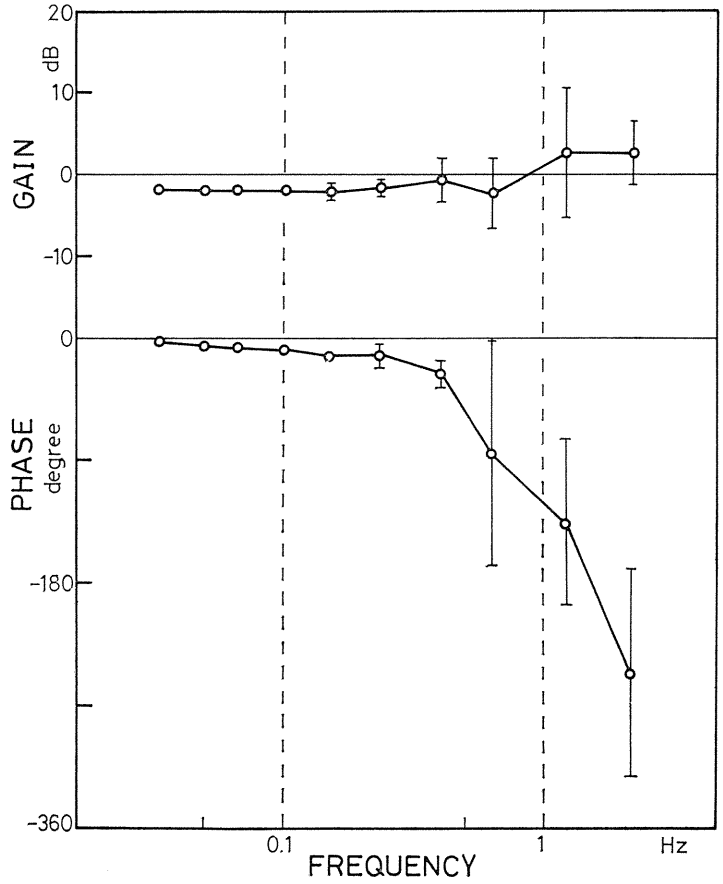

Fig. 3. 2. Closed-loop frequency response for random appearing input signal.

input. Fig. 3.2 gives the closed-loop input-output frequency response on tracking the random appearing input which is composed of 10 sine waves of different frequencies and random phases and has cut-off frequency at 0.4 Hz. As shown in the figure, the phase lag is about 110 degrees at 1 Hz. This lag is mainly due to the reaction time lag (about 0.2 to 0.4 sec.) of the operator. In this case, the tracking behavior of the human operator is in predictive control. On the other hand, for the single sine wave, the phase lag is only 1.5 degrees even at 1 Hz, so that the operator compensates his reaction time lag almost completely.

If the operator is an exact linear element, the output must not include the others except the input frequency. But it is really expected to include various frequency components due to the operator's irregular motions. Therefore, we computed error power spectra to define the frequency components. These are shown in Fig. 3.3 which are averaged over 10 trials. It can be seen that the input fre-

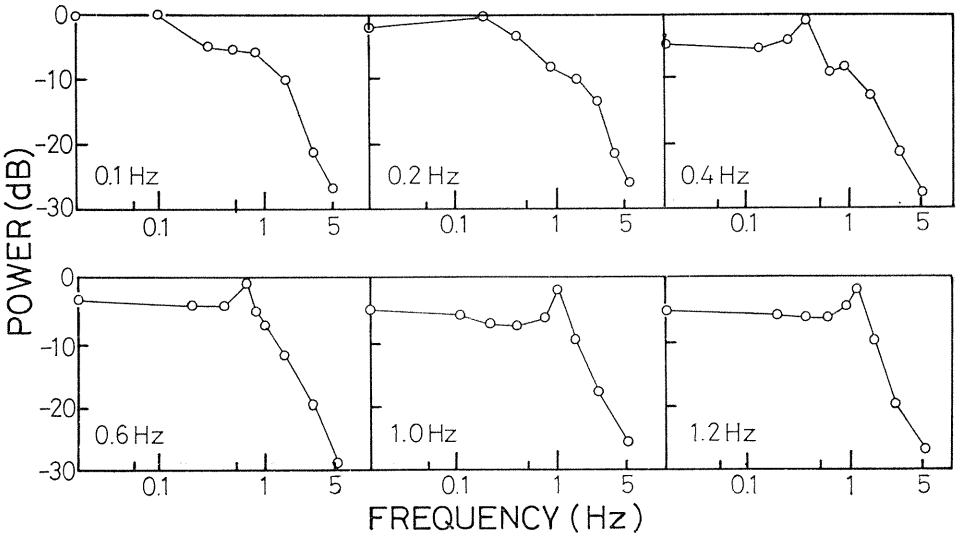

Fig. 3. 3. Error power spectra.

quency has much effect on the shape of the spectrum, i. e.;

(1) At low frequencies (0.1 Hz and 0.2 Hz), there is a broad band of power in the range to 0.5 Hz and both spectra have similar shape. Therefore, the error seems to come not from the phase shift at the input frequency but from the inaccurate motions in the neuromuscular system.

(2) As the input frequency is further increased, the error power at or near the input frequency increases and there appears peak of power which is centered at the input frequency. This denotes that the error is due to mistuning the input frequency.

Consequently, at single sine wave tracking, it is concluded that the trained operator generates, in a precognitive mode, a sine wave of frequency approximately equal to the input and then attempts to synchronize it with the input signal, for errors in synchronization or motor control.

3. 3. 2. two sine waves tracking

Six kinds of the inputs were tracked and the experimental results are shown in Table 3. 2. The values are averaged over 10 trials, too. At the inputs composed

Table 3. 2. Two sine waves tracking (averaged over 10 trials).

Input	I		II		III		IV		V		VI	
Frequency components (f_i) Hz	0.1	0.2	0.2	0.4	0.4	0.6	0.4	1.0	0.6	1.0	0.1	1.0
Input-output amplitude ratio (g)	1.1	1.2	1.2	1.3	1.2	1.3	0.7	0.9	0.7	0.9	1.0	0.8
Input-output phase difference (φ) and standard deviation	−1.8° ±0.3	−2.0° ±1.8	0.8° ±1.4	−3.5° ±0.6	0.1° ±1.6	−3.0° ±1.3	−1.7° ±2.7	-11.0° ±3.4	−5.9° ±2.9	−17° ±2.8	−8.2° ±2.3	−13° ±31
τ (sec)	−0.05	−0.03	0.01	−0.02	0.0	−0.01	−0.01	−0.03	−0.03	−0.05	−0.23	−0.04
Phase delays in predictive behaviors (from Fig. 3. 2.)	−7°	−15°	−15°	−30°	−30°	−75°	−30°	−110°	−75°	−110°	−7°	−110°
Mean square value (S_e)	0.03		0.06		0.05		0.21		0.14		0.06	

of two sine waves with the frequencies up to 0.6 Hz, the phase lags are very small and the amplitude ratios are restricted within the range from 1.1 to 1.3. It should be then emphasized that the operator's attention is consciously turned to both of two frequency components and he attempts to synchronize his output with the input in its totality. In this case, he seems to be in the precognitive mode similar to the single sine wave input.

The tracking behaviors at the inputs composed of two sine waves of 1 Hz and another frequency are considerbly different from the above. For example, at the sine waves of 1 Hz and 0.1 Hz, the operator tracks each sine weve one by one since there is a large difference between the frequencies. Whereas the phase and the amplitude at 1 Hz coincide with those of the input, the phase at 0.1 Hz is considerably delayed and then the time lag becomes 0.23 sec. As the above, when the frequencies are composed separate, the operator's attention is paid to the higher froquency and his output is synchronized with it in a predictive mode. Consequently, in case there is a large difference between the frequencies, the higher frequency component is tracked precognitively and the lower one is tracked predictively.

3. 3. 3. Three Sine Waves Tracking

Four kinds of the inputs were tracked and the experimental results are shown in Table 3. 3, in which the values in the column of 0.05 Hz were unable to be computed since the computer momory was insufficient.

At the input composed of the sine waves of 0.05 Hz, 0.1 Hz and 0.2 Hz, the human operator can make the phase and the amplitude coincide with the input signal

Table 3. 3. Three sine waves tracking (averaged over 10 trials).

Input	I			II			III			IV		
Frequency components (f_i) Hz	0.05	0.1	0.2	0.2	0.4	0.6	0.6	1.0	1.2	0.1	0.4	1.0
Input-output amplitude ratio (g)	—	1.1	1.0	1.0	1.0	1.2	0.7	1.1	1.1	0.8	0.8	1.4
Input-output phase difference (φ)	—	2.5°	4.0°	−5.0°	−9.7°	-13.1°	22°	−6.8°	−18°	−8.6°	-15.0°	−6.1°
and standard deviation	—	±0.5	±0.7	±1.3	±1.7	±2.9	±2.9	±0.9	±13	±1.9	±3.5	±14
τ (sec)	—	0.07	0.06	−0.07	−0.07	−0.06	0.1	−0.02	−0.04	−0.24	−0.1	−0.02
Phase delays in predictive behaviors (from Fig. 3. 2.)	—	−7°	−15°	−15°	−30°	−75°	−75°	−110°	−130°	−7°	−30°	−110°
Mean square value (S_e)	0.11			0.05			0.23			0.12		

and so he appears to be in a precognitive mode. On the other hand, at the input of 0.2 Hz, 0.4 Hz and 0.6 Hz, the phase lags of the operator are strongly marked though they are less then the lags in a predictive mode. Therefore, it is difficult to be concluded that the input is tracked precognitively. In case where the input is composed of the sine waves of higher frequencies (0.6 Hz, 1.0 Hz and 1.2 Hz), much attention is payed to the frequency components of 1.0 Hz and 1.2 Hz, but the frequency component of 0.6 Hz is almost neglected. Then, the amplitude ratio is less than the other two frequencies and there is a phase shift of 22°. This means that the response to the low frequencies are much affected by that to the high frequencies. When there is a large difference among the frequencies composed such as 0.1 Hz, 0.4 Hz and 1.0 Hz, the operator tracks each frequency component separately and the lowest frequency is tracked predictively and the highest frequency is tracked precognitively.

3. 4. Summary

We investigated how the tracking behaviors of the human operator varied from precognitive control to predictive control when sine waves of different frequencies were successively added more and more, and the following facts were pointed out:

(1) Single sine waves up to 1.2 Hz are tracked in a precognitive mode and at the same time, some closed-loop tracking seems always present to compensate for errors in prediction or additional disturbances.

(2) 2 sine waves up to 1.2 Hz are tracked in a precognitive mode if each frequency is closs by. But if both the frequencies are largely separated such as 0.1 Hz and 1.0 Hz, the high frequency component is tracked precognitively and the low frequency is tracked predictively.

(3) Even at 3 sine waves tracking, if the inputs are composed of sine waves of

only low frequencies, they are possible to be tracked precognitively. The other inputs are not the case. The human operator attempts to estimate some coherence on the input. He pays much attention to the special frequencies and tracks them in a precognitive mode. But the other frequencies are tracked in a predictive mode.

4. Control Structures of Precognitive Manual Tracking[40]

4. 1. Introduction

The purpose of this chapter is to mathematically describe precognitive control behaviors of the human operator in single sine wave tracking on the basis of the experimental results in the preceding chapter.

Here, some comments and hypotheses will be given as follows.

(1) In single sine wave tracking, the well-trained human operator is in a precognitive mode, i. e., has identified the input's regular repeating pattern and has had effectively complete information about the input's future. This means that the sine wave with the same frequency as the recognized input has been generated consciously by the operator.

(2) The human operator's output usually includes the other frequency components except the input frequency. They are called "remnant". We define human operator remnant as the portion of the operator's output that is not related to the system input by the output/input transfer function.[16] The remnant should therefore include the nonlinear, time-varying and random components of the operator's response.

It is experimentally revealed by *W. H. Levison et al.*[16] that the remnant obtained from manual control systems under the following situations reflects primarily the truly random component of the operator's response;

i) the controlled elements are linear,

ii) the task requirements are such that the subject apparently devotes continuous attention to the tracking task, and

iii) the subject manipulates a single control.

Then the remnant is assumed to arise form an equivalent observation white noise process.

Since our sine wave tracking experiment satisfies the above situations, the remnant so obtained should reflect primarily the random component originating from the sources within the human operator. The experimental results show that the frequency of the sine wave has much effect on the shapes of the error power spectra. Therefore we attempt to represent the remnant by two equivalent noise processes which are mutually independent gaussian white noise processes. They are named "*motor noise*" and "*synchronous noise*" respectively. The former corresponds to the inaccurate motion in the neuromuscular system at the low input frequencies and the latter corresponds to the random phase shift at the high input frequencies.

(3) It should be noted that the reaction time delay due to physiological limitations is completely compensated for as shown in Table 3. 1.

4. 2. Modeling of Precognitive Tracking Tasks

Let's now consider a model for the human precognitive control. The human

operator in a precognitive mode seems to have the same dynamics as the command generator which generates the input signal. Then we assume that the operator's characteristics are approximately represented by the three linear subsystems as shown in Fig. 4. 1.

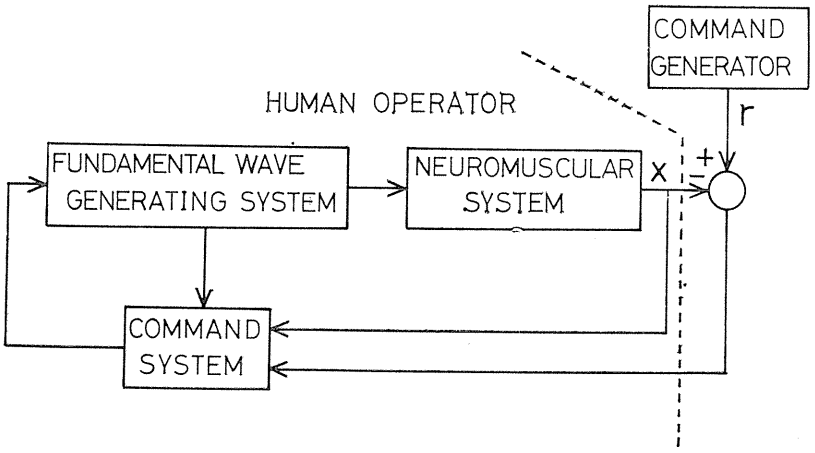

Fig. 4. 1. Schematic model of the operator in single sine wave tracking.

(I) *Fundamental wave generating system*: this has the same dynamics as the command generator and sends forth the signal with the frequency equivalent to the input signal, but is not capable of adjusting the phase and the amplitude to the input signal.

(II) *Neuromuscular system*: this is often approximated linearly by an adjustable first-order lag.

(III) *Command system*: this deals with the signals from the internal subsystems and the external display, and sends control signals to the fundamental wave generating system in order to synchronize with the input signal.

The command generator, sub system (I) and (II) can be represented by differential equations as follows.

* *Command generator*:

$$\begin{cases} \dot{z}_1 = \omega_0 z_2 \\ \dot{z}_2 = -\omega_0 z_1. \end{cases} \tag{4—1}$$

* *Neuromuscular system*:

$$\dot{x} = ax + gu_1. \tag{4—2}$$

where x is the operator's output, and a and g are parameters.

* *Fundamental wave generating system*:

$$\begin{cases} \dot{u}_1 = -\omega_0 u_2 \\ \dot{u}_2 = \omega_0 u_1 + bu_c. \end{cases} \tag{4—3}$$

Since Eqs. (4—1), (4—2) and (4—3) correspond to Eqs. (2—1), (2—7) and (2—8) respectively, these equations can then be solved as a servo problem. The performance index is defined by

$$J=\int_0^\infty \{(r-x)^2+\rho u_c^2\}dt. \tag{4—4}$$

This is based on the assumption that the human operator behaves so as to reduce both the error e and the control effort u_c. By using this performance index, the resultant closed-loop system becomes a linear system which represents the human operator's responses successfully and the parameters of the control system are determined by only one parameter, ρ.

Then from Eq. (2—25) the command system can be represented as

$$u_c=c_1z_1+c_2z_2+c_3x+c_4u_1+c_5u_2, \tag{4—4}$$

where

$$c_1=\rho^{-1}b\omega_0{}^2gk_5,$$

$$c_2=-\rho^{-1}b\omega_0g(k_3-\omega_0{}^2k_6),$$

$$c_3=\rho^{-1}b\omega_0g(k_3+ak_5+a^2k_6),$$

$$c_4=-\rho^{-1}b\omega_0{}^2g^2k_6,$$

$$c_5=\rho^{-1}b\omega_0g^2(k_5+ak_6),$$

and $K=\begin{pmatrix} k_1 & k_2 & k_3 \\ k_2 & k_4 & k_5 \\ k_3 & k_5 & k_6 \end{pmatrix}$ is the solution of Riccati equation.

Now, x, u_1 and u_2 which are the variables internal to the model are directly available. The input signal $z_2=r$ is obtained as $z_2=e+x$, where e is the displayed

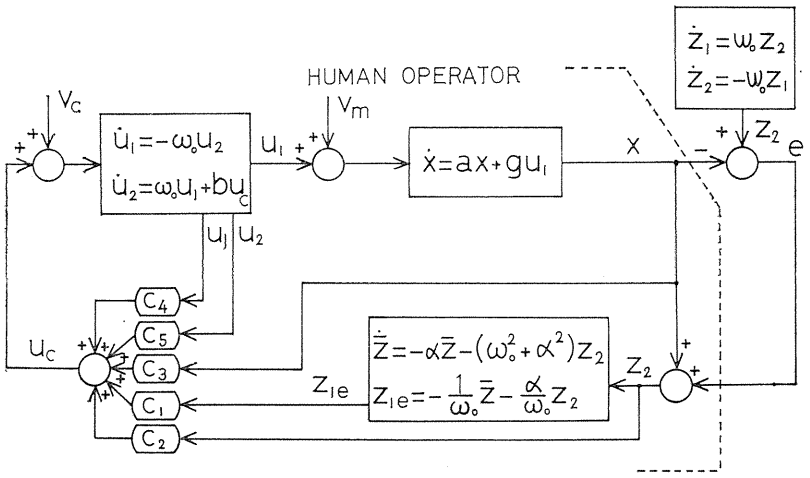

Fig. 4. 2. Structual model of the operator in single sine wave tracking.

error and x is the operator's output. But z_1 must be estimated from z_2.

Using the observer, the estimate z_{1e} of z_1 is obtained as

$$\begin{aligned}\dot{\bar{z}} &= -\alpha\bar{z} - (\omega_0{}^2+\alpha^2)z_2,\\ z_{1e} &= -\frac{1}{\omega_0}\bar{z} - \frac{\alpha}{\omega_0}z_2,\end{aligned} \tag{4—5}$$

where α is an arbitrary parameter of the observer. This represents the human operator's perception of velocity from the position of the input signal. The model for the operator's linear responses has now been completed. (see Fig 4. 2)

4. 3. Remnant model

We attempt to represent the remnant by two additive noise processes, motor noise and synchronous noise, which are mutually independent zero-mean gaussian white noises. In Fig. 4. 2, v_m represents motor noise added to the neuromuscular system and v_e represents synchronous noise added to the output of the synchronous command system. In this case, the linear response model must be solved as the linear servo problem with moise where the performance index defined by

$$J = E\left[\int_0^\infty \{(z_2-x)^2+\rho u_c{}^2\}\,dt\right], \tag{4—6}$$

is minimized. It is known that the solution to this problem is the same as the solution with no noise if v_m is zero-mean gaussian white noise.

The power spectra of the output x of the model for v_m and v_c are

$$\Phi_m(\omega) = N_m\frac{[-\omega^2+\omega_0{}^2(1-c_5)]^2+(c_4\omega_0\omega)^2}{A^2+B^2}, \tag{4—7}$$

$$\Phi_c(\omega) = N_c\frac{1}{A^2+B^2}, \tag{4—8}$$

where

$$\begin{aligned}A &= -(T_N C_4\omega_0+1)\omega^2+\omega_0{}^2(1-c_3-c_5),\\ B &= -T_N\omega^3+\{T_N\omega_0{}^2(1-c_5)+c_4\omega_0\}\omega,\\ T_N &= -1/a = 1/g,\quad b=-\omega_0,\end{aligned}$$

and N_m and N_c represent autocovariance of v_m and v_c respectively.

It is known that N_N is about $0.1 \sim 0.6$ sec.[3] N_m and N_c are arbitrary since the magnitudes of the remnant power are not considered here. And T_N, ρ and h are chosen so that $\Phi_m(\omega)$ for low frequency input signals, $\Phi_c(\omega)$ for high frequency input signals and $\Phi_m(\omega)+h\Phi_c(\omega)$ (h is a constant) for intermediate frequency input signals respectively coincide with the experimental error power spectral densities. They are shown in Table 4. 1. As the input frequency is increased, T_N is decreased. When the input frequency is higher, the operator has to respond more quickly and as the result, the cutoff frequency in the neuromuscular system must be increased. Fig. 4. 3 shows the theoretical and experimental error power spectral densities at three frequencies in Table 4. 1. As an example, Fig. 4. 4 shows the

responses of both the model and the human operator at input frequency 1.2 Hz. The response of the model was simulated by analog computer and then the gaussian white noise was approximated by the sum of many sine-waves.

Table. 4. 1. The values of model parameters.

Input frequency	T_N	ρ	h
0.1 Hz	0.6	1	—
0.4 Hz	0.1	1	4
1.2 Hz	0.1	1	—

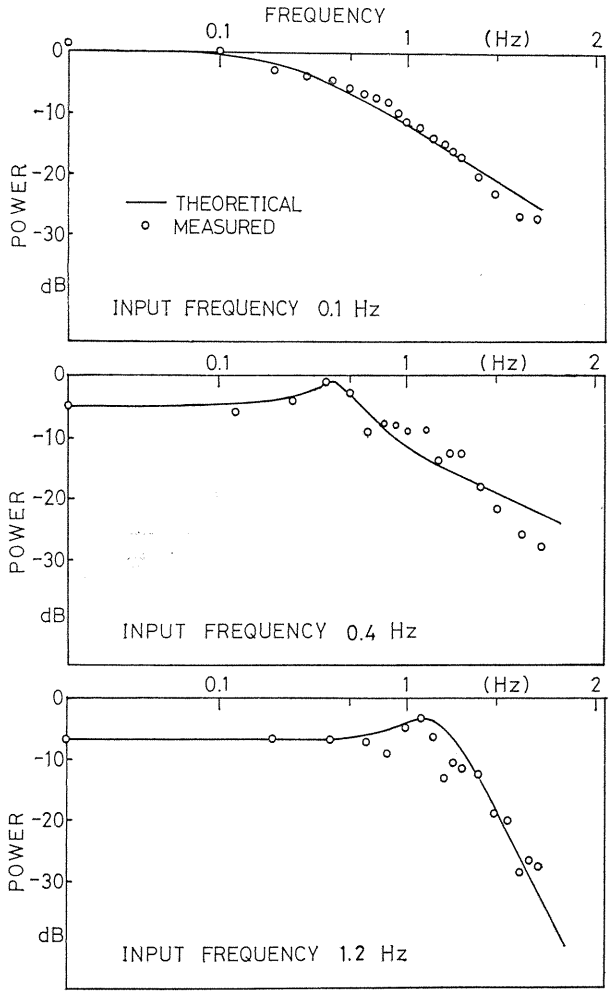

Fig. 4. 3. Normalized injected remnant spectra and the comparison with the measured error power spectra.

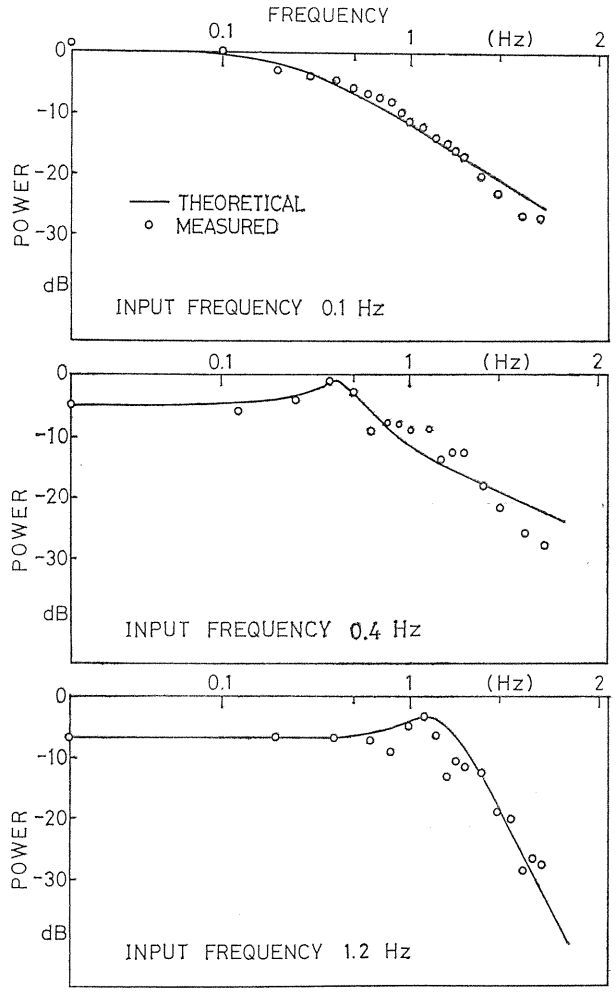

Fig. 4. 4. Experimental and model sine wave tracking runs (input frequency 1.2 Hz).

4. 4. Summary

On the assumption that the well-trained operator has consciously formed, internal to himself, the same dynamics as the command generator which was considered to generate the input signal, a linear control model was constructed mathematically. Then, the precognitive tracking behaviors of the human operator were represented by the linear model plus the remnant. The remnant was modeled by mutually independent gaussian white noises, i. e., motor noise and synchronous noise,

The linear precognitive model proposed is not applicable to the case that even if the reference input has the regular repeating pattern (high coherence), it doesn't fall within the response functions of the command generator, such as periodic square waves. If the input function is substituted for another similar differentiable function, however, it is possible to construct the linear precognitive control model. For

example, note that we will be able to expand the input function in terms of a finite Fourier series.

When the input is composed of four and more sine waves, the operator is unable to detect the input's coherence and tracks it in a predictive mode. Then, the predictive control system has to be constructed.

5. Forced-paced Preview Manual Tracking[41]

5. 1. Introduction

In the present and next chapter, we discuss the cases where the operator can see the future input as well as the present one, i. e., preview manual tracking tasks and analyze how the operator processes the information about the future input.

It is essential at the ceginning to classify preview into two types of control, i. e., forced and self-paced controls.[2] Now, consider a function in space $y(x)$ which represents a reference input or cource for a given control system. If for some reason we traverse the course with constant velocity, then the task is called "*forced-paced*" and the reference input $y(x)$ is regarded as equivalent to $y(t)$. In most human tasks of the sort we are considering, the operator is able to control his speed when traversing a course; then the task is called "*self-paced*". The present chapter will assume forced-pacing to develop the principal ideas. Self-pacing is considered in the following chapter.

5. 2. Experiments

5. 2. 1. Experimental arrangement

The outline of the experimantal arrangement is depicted in Fig. 5. 1. A 20-cm industrial TV receiver is used to indicate to the the operator the present and future values of the input functions. On the TV screen the operator sees the input

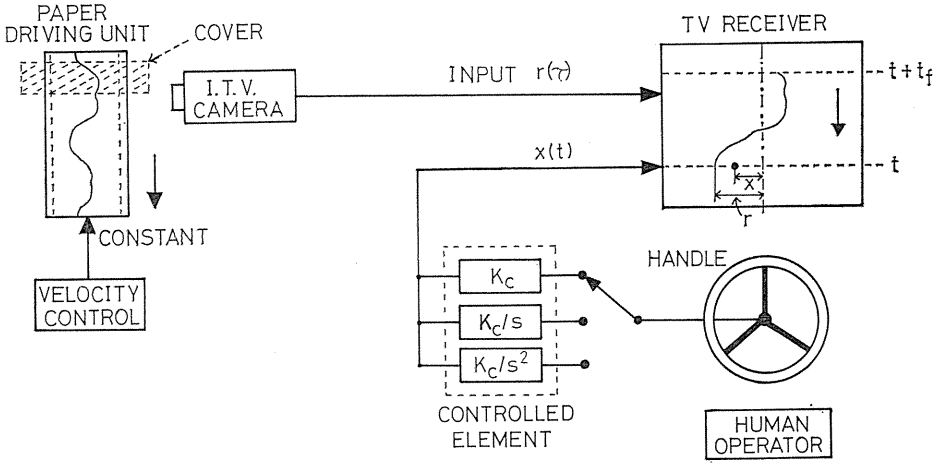

Fig. 5. 1. Experimental arrangement of preview manual tracking.

function from the current time t to the preview time t_f and the spot as the output of the controlled element. The input function moves up and down as time passes. The spot moves right and left according to the output of the controlled element. The maximum amplitude of the input function is set to cover 80 % of the horizontal width of the screen for easier view by the operator.

The input function is sent through the TV camera. Attached to the paper feeding device is an endless belt of length 2035 mm and width 200 mm. The paper on which the input function is written is pasted to the belt. The belt is rotated at a constant speed. The rotating speed for the experiment is set to one revolution per 60 sec. The accelerator is not yet used because we assume forced-paced control. The position of the TV camera is adjusted such that the distance between the position of the spot and the upper end of the TV screen is equal to the maximum preview time (1.5 sec). Furthermore, a shield board is inserted between the belt and TV camera to alter the preview time. The manipulator is a steering wheel of an automobile, 38 cm in diameter, which has a negligible friction and to which a potentiometer is connected directly.

Three types of controlled element, i. e., pure gain $G_c(s)=K_c$, integration K_c/s, and double integration K_c/s^2, are used. In view of the human operator's reaction time of 0.2 to 0.4 sec, six preview times, $t_f=0.0$, 0.25, 0.5, 0.75, 1.0, and 1.5 sec are used.

The input function has to be a smooth and random appearing signal. In the present experiment, the input function consists of the superposition of 10 sine waves of all different frequencies and random phases. The frequencies range from 0.209 rad/sec to 13.8 rad/sec, which are roughly equally spaced on a log scale. The sine waves of frequencies from 0.209 rad/sec to 2.51 rad/sec have the same amplitude and for the waves of frequencies higher than 3.98 rad/sec, the amplitude is reduced to one-tenth the amplitude of the waves of lower frequencies in order to smooth the signal.[3]

The waveform of the input function can be expanded or contracted in the direction of movement, but by changing the speed of the belt, the frequency characteristics of the change of the waveform. In the compensatory tracking behavior, only the present value of the input function is shown. Therefore, the input function seems to remain unchanged despite the change in waveform, and the human tracking characteristic will not change either. In the preview behavior in which the future waveform is also shown, it is doubtful that the same tracking characteristic will be obtained when the change in the waveform is large since the human visual response for a high or low speed object is not always linear. However, since the objective of the present experiment is to establish the relation between preview time and tracking behavior, the speed of the belt is determined so as to facilitate the operator's observation. The investigation on the speed of the belt appears to be very important.

5. 2. 2. Experimental Procedure

The operator was instructed to track the waveform on the screen as close as possible to minimize errors. Each trial was conducted for 120 sec. The operator was trained to reach a stable level of a performance measure. The experiments were done for 18 combinations of preview times and controlled elements. For each such combination, two operators were asked to perform the trials.

It has been possible in conventional compensatory control systems to obtain the transfer function associated with the operator directly. In the preview control system, however, since the operator can see the future input and the present output, it is impossible to directly determine the open-loop describing function of the operator. In the present experiments, therefore, the closed-loop frequency responses from the input function $r(t)$ to output $x(t)$ are measured and based on the results, the tracking characteristics of the operator are estimated. Since the input function is periodic and, furthermore, since its frequency components are known, the closed-loop frequency response $G(j\omega)$ can be computed by

$$G(j\omega)=\frac{X(j\omega)}{R(j\omega)}, \qquad (5-1)$$

where $R(j\omega)$ and $X(j\omega)$ are the Fourier transforms of the input function $r(t)$ and output $x(t)$.

5. 3. Experimental Results

5. 3. 1. Effect of preview times on closed-loop frequency responses

The closed-loop frequency responses were obtained for each controlled element and preview time based on five runs after the operator becomes skilled. Since the variation of the frequency responses between runs and between the operators was small, the average values were calculated over 10 trials (5 trials by each operator). Fig. 5. 2 shows the effect of preview times on closed-loop frequency responses for three differenct controlled elements.

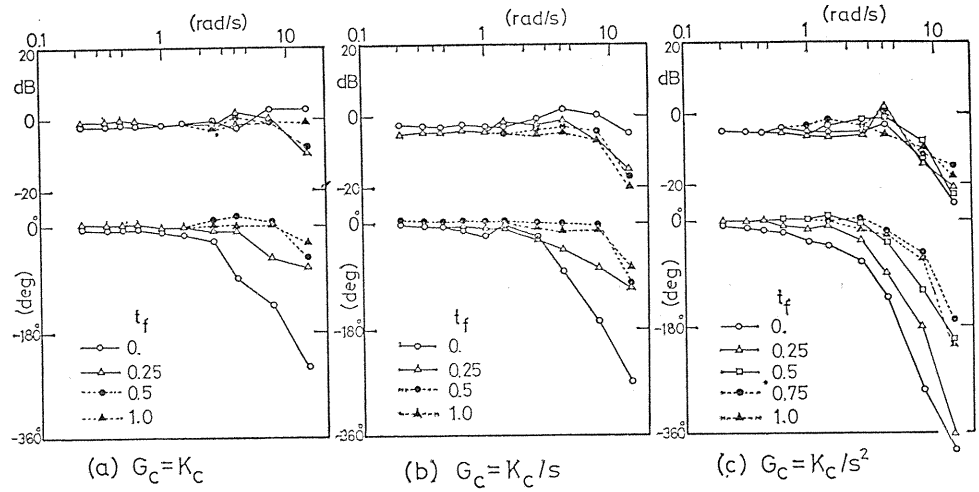

Fig. 5. 2. Effect of preview times on closed-loop frequency responses.

If the future value of the input function is known, the operator can react to the changes in advance. The influence of the reaction can be seen more distinctively in the phase characteristic than in the gain characteristic regardless of controlled elements. That is, it can be seen that the operator tries mainly to compensate the delay in the phase rather than the gain by seeing the future value. It can be seen

also that the phase characteristic is improved as the preview time becomes longer but it does not change much beyond a certain preview time. This "critical" preview time tends to be longer as the order of the controlled element increases such as 0.5 sec for K_C, 0.5 sec for K_C/s and 0.75 sec for K_C/s^2. Therefore, it is necessary for the operator to see further ahead in order to compensate the phase difference since the phase delay becomes longer as the order of the controlled element increases.

5. 3. 2. Effect of preview times on the control performance

For each trial, normalized mean squared errors was computed.

$$S=\int_0^{120} e^2dt/\int_0^{120} r^2dt, \tag{5—2}$$

where r is the input function and e is the error. Fig. 5. 3 shows the effect of

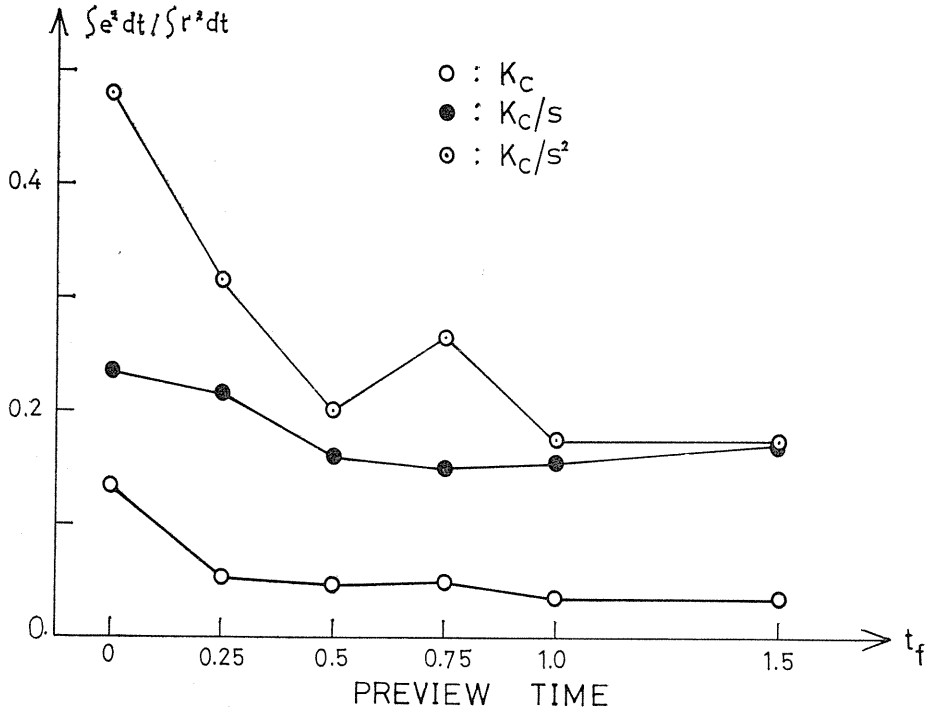

Fig. 5. 3. Effect of preview times on the control result.

preview time on the control performance for three controlled elements (average values over 10 trials, 5 trials by each operator). Regardless of preview times, the conrol performance becomes worse as the order of the controlled element increases.

There is a peak at $t_f=0.75$ in the curve corresponding to K_C/s^2. This is because of one of the operator's very poor reaction in this test and should not influence the results. The control performance becomes constant when the preview time is 0.25 sec for K_C, 0.5 sec for K_C/s and 1.0 sec for K_C/s^2. This phenomenon is in good correspondence with the result obtained in section 5. 3. 1.

5. 4. Preview Model and Weighting Function into the Future

Sheridan proposed three preview control models by theoretically considering the preview behavior of human operators in driving automobiles and flying airplanes.[2] In this paper, only one of the models using extended convolution integral is considered since it is deeply associated with the present research. The essential point in this model lies in the sum of the convolution integral on control error $e(t)$ and the convolution on the future value of the input function, given by

$$u(t)=\int_0^{T_m} e(t-\tau)w_m(\tau)d\tau+\int_{-t_f}^{T_m} r(t-\tau)w_p(\tau)d\tau, \qquad (5\text{—}3)$$

where $w_m(\tau)$ denotes the weighting function associated with an operator for error e, $w_p(\tau)$ the weighting function for the future value of input function, T_m the memory limit of weighting function and t_f preview time. The block diagram of the preview control model is shown in Fig. 5. 4, where G_A is the transfer function corresponding to the second term in Eq. (5—3) and G_B is that corresponding to the first term. But the forms of weighting functions $w_m(\tau)$ and $w_p(\tau)$ were not considered.

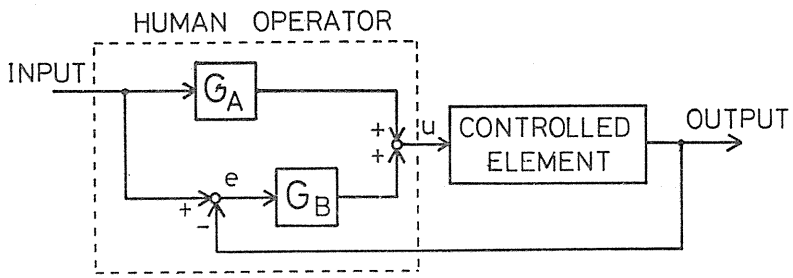

Fig. 5. 4. Preview control model by Sheridan.

Fig. 5. 5 is the preview control system[25] which has been proposed in chapter 2. In this control system the tracking characteristic is improved as the preview time of the future value is prolonged. However, the effect of making t_f large is

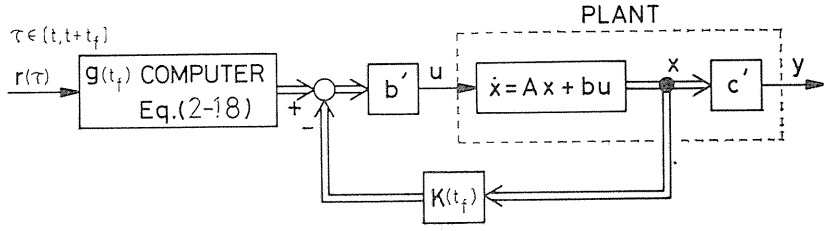

Fig. 5. 5. Preview cotrol system (see Fig. 2. 3.).

not very great. It has been shown that it is sufficient to measure the future value up to just beyond the time of peak of the impulse response of the closed-loop system. One of the distinct characteristics of the system is the phase lead in a

high frequency region. Fig. 5. 6 shows the frequency responses for the second-order controlled element.

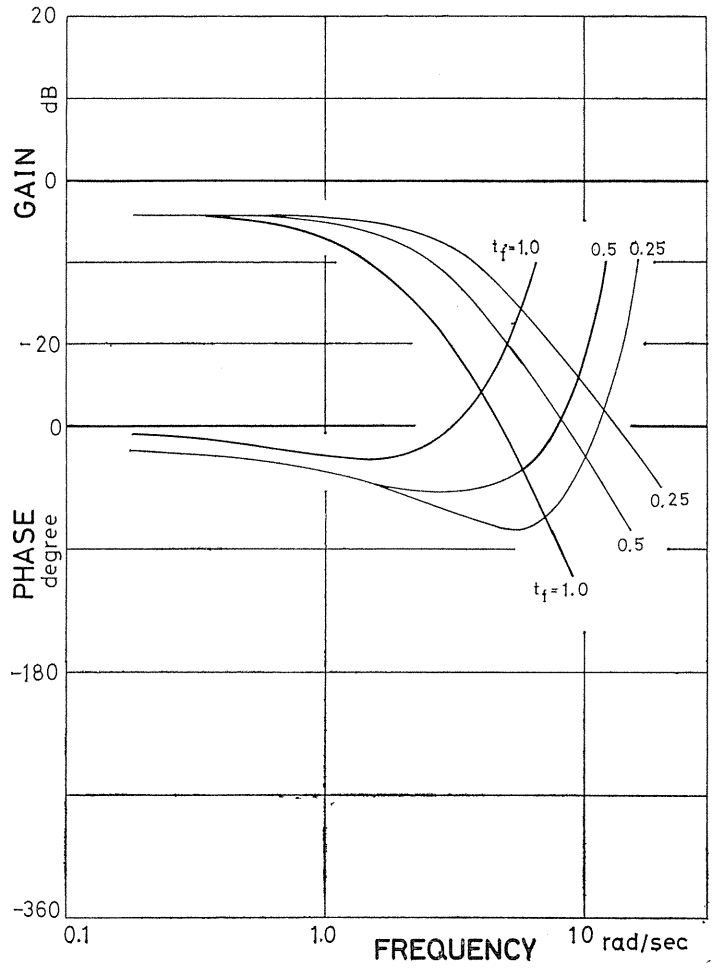

Fig. 5. 6. Frequency response of the preview control system (second-order plant).

Now we propose a new preview control model and consider the weighting on the future value of the input function. Here note that preview of the input has an essential effect on the phase compensation of the operator. Therefore, we assume that the preview behavior of the operator is formally represented by two blocks as shown in Fig. 5. 7, where the blocks internal to the operator are enclosed by a broken line. The feedfoward block $G_F(s)$ processes the future value of the input. The block $G_P(s)$ in the closed-loop operates on the perceived error. It is further assumed that;

(1) the closed-loop portion depends on the input and the controlled element, and never on the preview time,

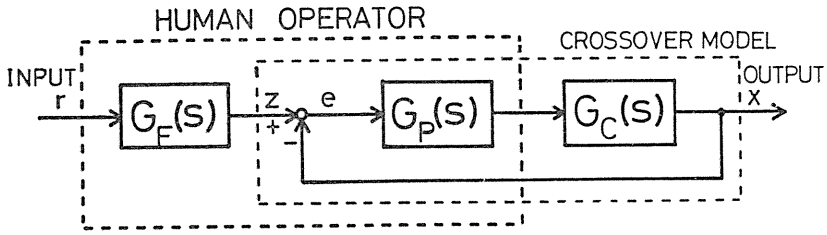

Fig. 5. 7. Block diagram for forced-paced preview control model.

(2) $G_F(s)$ serves to lead the phase, and
(3) the output of $G_C(s)$ is fed back sorely for the recognition of the error, i. e., the feedback loop is single.

When $t_f=0$, $G_F(s)$ should be unity. Then, the closed-loop portion is equivalent to a compensatory tracking system and can be approximately represented by the model of the operator with unpredictable type inputs. There have been many models for compensatory tracking systems. The crossover model proposed by *McRuer et al.*[15] shall be used here (see Eq. (1—4) in chapter 1). It is the most representative and simplest of all the models.

$$G_P(s)\cdot G_C(s)=\frac{\omega_c\cdot e^{-\tau_e s}}{s}, \tag{5—4}$$

where $\omega_c=3\sim5$ rad/sec, $\tau_e=0.15\sim0.35$ sec. Once the chracteristics of the input function and controlled element are determined, the form of the closed-loop portion in the model can be established.

The feedfoward block $G_F(s)$ is defined as follows:

$$G_F(s)=\int_{0-}^{t_f} w_{t_f}(t')e^{t's}dt', \tag{5—5}$$

where $w_{t_f}(t')$ is to be replaced by delta function if $t_f=0$. Therefore, $G_F(s)=1$, when $t_f=0$.

It follows from Eq. (5—5) that the relation between $R(s)$ and $Z(s)$ in Fig. 5. 7 is given by

$$Z(s)=\int_{0-}^{t_f} w_{t_f}(t')e^{t's}dt'R(s). \tag{5—6}$$

The integration may be approximated by the following sum:

$$Z(s)=\sum_{i=0}^{N} w_{t_f}(i\Delta t)e^{i\Delta t}\Delta t R(s), \tag{5—7}$$

where $t_f=N\Delta t$. The inverse Laplace transform of Eq. (5—7) is given by

$$z(t)=\sum_{i=0}^{N} w_{t_f}(i\Delta t)r(t+i\Delta t)\Delta t. \tag{5—8}$$

Equation (5—8) implies that the present value $z(t)$ is the sum of future input values times the weight w_{t_f}. The integral form of Eq. (5—8) may be given by

$$z(t)=\int_0^{t_f} w_{t_f}(t')r(t+t')dt'. \tag{5-9}$$

Letting $t+t'=\tau$, the above integration can be rewritten as

$$z(t)=\int_t^{t+t_f} w_{t_f}(\tau-t)r(\tau)d\tau. \tag{5-10}$$

It should be noticed that the present model is different from the extended convolution model given by *Sheridan* in Fig. 5. 4. It is possible to perform equivalent transformation on Fig. 5. 4 to make it in the form of Fig. 5. 7, but the resultant block corresponding to the feedfoward block takes a form different from $G_F(s)$ in Fig. 5. 7.

The shapes of the weighting function w_{t_f} can be determined from the experimental results. As mentioned previously, it was found from the experimental results that the gain characteristic did not change much but the phase lead was great when the preview time was prolonged. That is, the gain characteristics could be seen as constant regardless of the preview time. The closed-loop portion containing $G_P(s)$ is replaced by the closed-loop describing function for compensatory tracking. Then, the procedure to determine w_{t_f} is as follows; first, we compute the difference (i. e. the phase lead) between the phase characteristic at each preview and that for compensatory tracking, and next we determine, through the trial and error method, the shape of w_{t_f} so as to compensate its phase lead. The

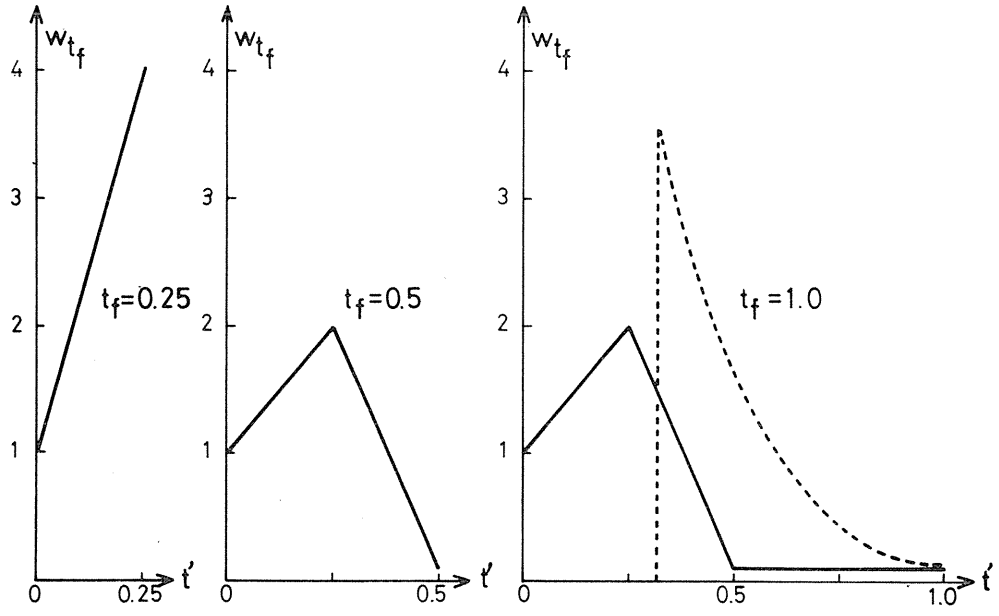

WEIGHTING FUNCTIONS

Fig. 5. 8. Dependence of weighting functions on preview times.

forms of weighting functions for various preview times are shown in Fig. 5. 8. The weights are normalized in such a way that they have unity for the present value of input function and approximately graphed using the straight line segments. The gain characteristic of $G_F(s)$ is almost constant throughout and therefore its influence on the gain of the total system is negligible.

Since the weighting function w_{t_f} has a peak value at around $t'=0.25$ sec and exhibit low values beyond $t'=0.5$ sec, it can be judged that the operator pays special attention at around $t'=0.25$ sec and does not pay much attention beyond $t'=0.5$ sec. This signifies that the operator can obtain the amount of lead necessary to compensate the phase delay of himself and the controlled element when he sees ahead slightly beyond $t'=0.5$ sec.

The dotted line in the figure shows the impulse response of the closed-loop portion when the crossover model is used. The parameters in Eq. (5—4) are chosen such that $\omega_c=5.5$ and $\tau_e=0.33$ sec. The peak of the impulse response occurs at around the preview time at which the value of the weighting function becomes small. Therefore, it is sufficient for the operator to see the future value slightly beyond the preview time at which the peak of the impulse response of the closed-loop portion, i. e., in compensatory tracking system occurs. In the preview control system in chapter 2, the form of the weighting function into the future input is that of the impulse response of the closed-loop portion in the block diaglam of Fig. 5. 5. The difference between the weighting function w_{t_f} and the theoretical result is in the treatment of weights for the present value of input function.

If the operator could have tracked with complete adjustment of his own characteristics, the operator may be able to follow the input function with satisfactory accuracy and does not necessarily need to see the present value since he has seen the future value of the input function beforehand. In practice, however, the operator's adjustment is not complete and unpredictable disturbances will exist. Therefore some compensation is necessary. This means that the operator's utilization of the present value is nothing more than checking his own imperfectness of behavior.

In this way, the preview tracking behavior of the operator is composed of the feedfoward block to process the future input and the feedback loop to compensate uncertainty of his behavior. On the other hand, since the theoretical preview control system does not utilize the present value of the input function, the system is essentially a feedfoward control. In effect, if the weight for the present value is changed from 1 to 0 in Fig. 5. 8, the closed-loop frequency response has lead phase at high frequency and is different from the experimental results.

When $t_f=0.25$ sec, the weight for the future value is relatively very large compared to the weights for other preview times. This means that when the preview time is short, the emphasis is on the compensation of the phase delay of himself and the controlled element rather than on checking the present error. Therefore, the preview behavior is closer to feedfoward control.

Fig. 5. 9 shows the frequency response of the total system with the weighting function w_{t_f} determined as above and the comparison with the measured closed-loop frequency response. The experimental date are well fitted by the preview model over a wide frequency range for $G_c(s)=K_c$ and K_c/s. But when the controlled element is K_c/s^2 and $t_f=1.0$ sec, the theoretical gain curve at high frequencies is considerably lower than the curve obtained from the experiment. This may be explained as follows: for the higher order controlled element and a longer preview,

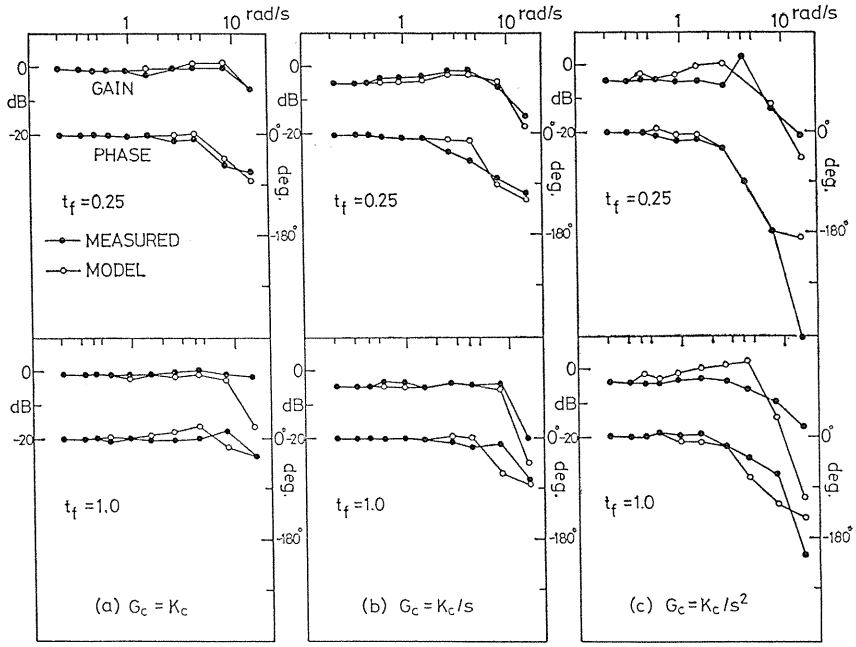

Fig. 5. 9. The frequency responses of the total system with the weighting function W_{tf} and the comparison with the measured closed-loop frequency responses.

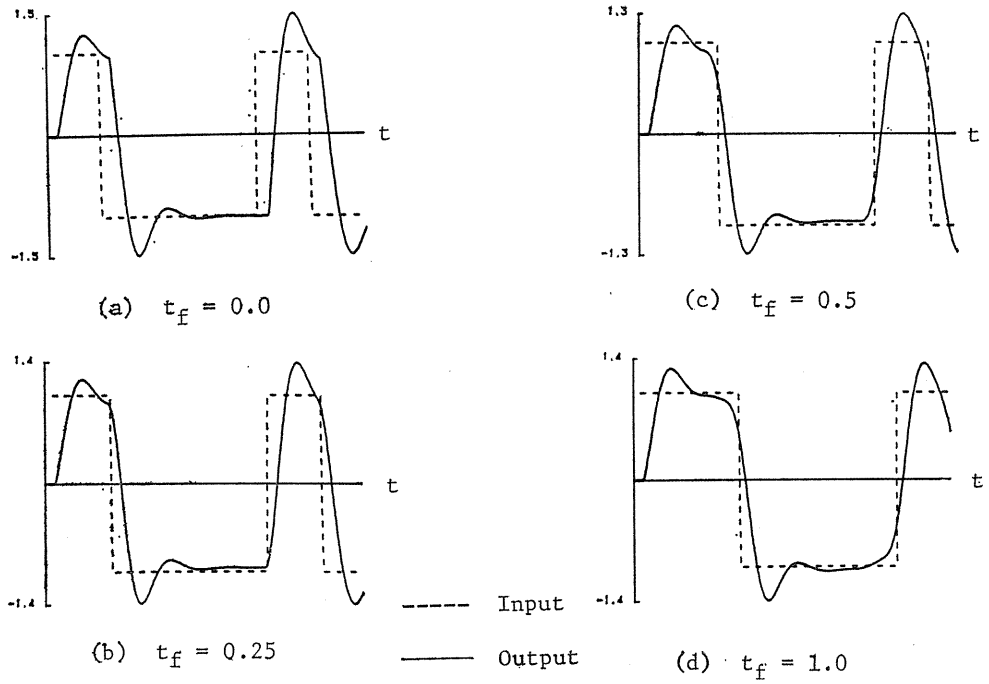

Fig. 5. 10. The step responses of the preview control model (preview times : t_f=0, 0.25, 0.5, 1.0 sec).

the operator changes the compensatory behavior itself and then the assumption that the closed-loop portion is invariant with preview time no longer holds.

Fig. 5. 10 shows the step response of the preview control model proposed. $G_F(s)$ is defined by Eq. (5—5). $G_P(s)\cdot G_C(s)$ is modeled by the crossover model represented by Eq. (5—4), where $\omega_c=3.5$ rad/sec and $\tau_e=0.2$ sec. In the figure, the broken line is input and the solid line is output. It is illustrated that the future input has much effect on improving the tracking characteristics, especially compensating the time lag. Fig. 5. 11 shows the actual input $r(t)$ (the broken line)

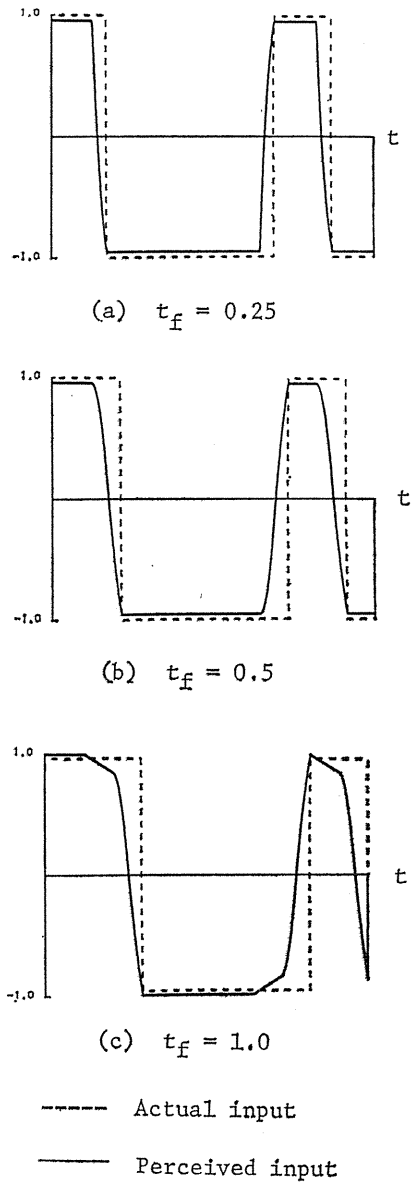

Fig. 5. 11. The actual input $r(t)$ and the perceived input $z(t)$ of the preview control model.

and the preceived input $z(t)$ (the solid line) of the preview control model. The operator attempts to track the input $z(t)$ which has been modefied by the weighting function w_{tf}.

5. 5. *Summary*

In operating automobiles, a driver exhibits an excellent tracking control because he can see the road ahead. In this chapter, basic experiments on the forced-paced preview control using a simple simulation device have been made and the following conclusions have been drawn:

(1) The utilization of the future input by the operator has much effect on the phase compensation of the tracking characteristics. However, there is a limit to the effective compensation even when the preview time is made long. The phase characteristics can be improved up to a certain preview time, but it is not made better after that. This "critical" preview time tends to be larger when the order of the controlled element is increased. A similar tendency can be seen in the relation between the preview time and mean square errors. Therefore, the improvement of the control error in the preview tracking is mainly due to compensation for the phase delay of the controlled element and his own.

(2) The preview behavior of the operator can be represented approximately by a model which consists of a series connection of the feedfoward block processing the input in the future and the closed-loop portion having compensatory behavior. Weighting functions of the operator for future value were determined based on the comparison between this model and the experimental results. The weighting function has a peak value at around $t_f=0.25$ sec and a very small value after $t_f=0.5$ sec. Since the peak of the impulse response of the closed-loop portion of the model occurs in the vicinity of $t_f=0.3$ sec, it is sufficient for the operator to see the future value slightly beyond the preview time at which the peak occurs.

(3) However, the preview behavior of the human operator is not a feedfoward control like the preview control system derived from control theory. Rather, it is a feedback control system with a touch of feedfoward because of its uncertainty. If the preview time is short, however, it has been found that the operator must behave as a feedfoward system to obtain the necessary phase lead.

6. Self-paced Preview Manual Tracking

6. 1. *Introduction*

We discuss the cases where the operator is able to see ahead and in addition, controls his speed when traversing a course. In particular, much attention is directed to how the operator processes the information about the future input in order to modulate his driving speed. It should be noted here that the human tracking tasks including both self-pacing and preview have scarcely been analyzed until now. (2), (10)

6. 2. *Experiment*

6. 2. 1. *Experimental arrangement*

The experimental arrangement is almost the same as shown in Fig. 5. 1. In

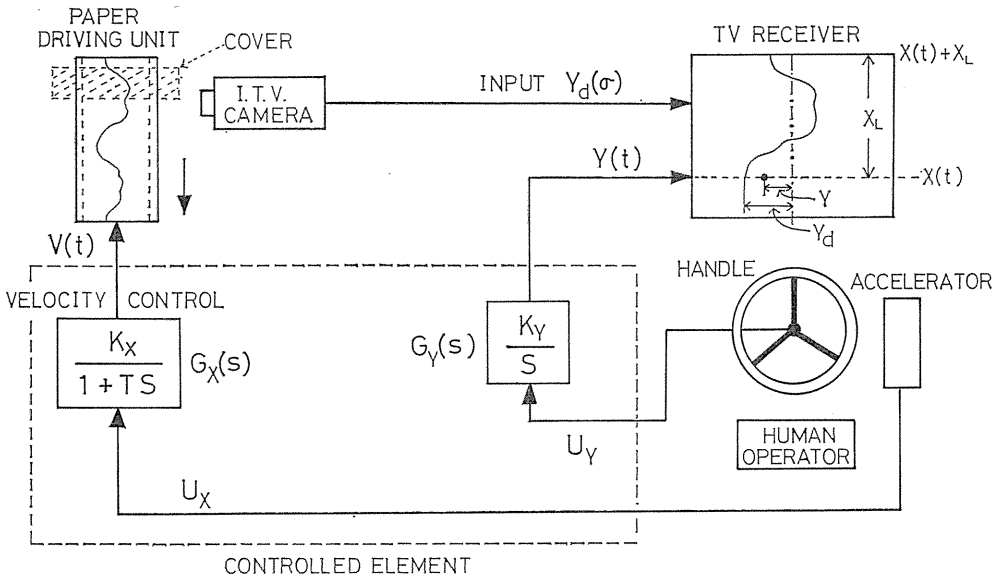

Fig. 6. 1. Experimental arrangement of self-paced preview tracking.

this case, however, the accelerator is used in order to control the tracking speeds (see Fig. 6. 1). The transfer characteristics of the velocity control unit which is driven by D. C. motor is approximately represented by the first-order lag ($G_X(s) = K_X/(1+Ts)$). On the other hand, the controlled element of the handle system is integration $G_Y(s) = K_Y/s$.

The input functions which were tracked are maximum length sequence (Y_M), trapezoid wave (Y_A), semicircle (Y_B), triangular wave (Y_C) and random signal (Y_D) (see Fig. 6. 2). The period N of maximum length sequence (M-sequence) is 31 and

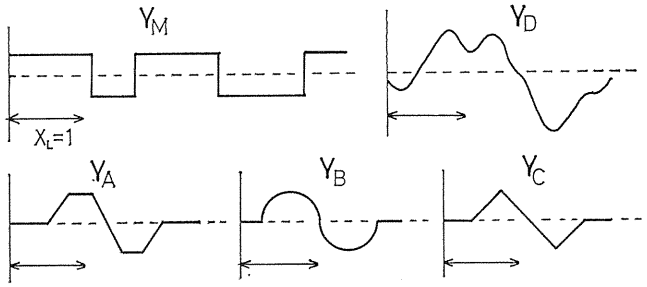

Fig. 6. 2. Inputs used in the experiments.

the minimum pulse width is 6 cm and the amplitude is 4 cm on the TV screen. The each amplitude of trapezoid wave, semicircle and triangular wave is 8 cm and the maximal one of random signal is 14 cm on the screen. These values are selected such that the human operator is able to smoothly operate the handle.

Three kinds of preview length, $X_L=1$, 1/2 and 1/3 are used. $X_L=1$, the length

of which is about 12 cm on the screen, means that the operator can see the whole of TV screen. The distance between the operator and TV screen is about 50 cm.

6. 2. 2. *Experimental procedure*

In conventional manual tracking tasks, there were many cases where the operator was instructed only to minimize the error displayed on the screen. But, since, in the present experiment, the operator is able to control his tracking speed, instructions as to only the error may induce undesirable results that the operator tracks the input at extreme low speeds. Therefore, it was necessary to provide some index concerning the tracking velocity. Considering this point, we adopted the following performance index in the present experiment and instructed the operator to make it as little as possible.

$$P.I.=E_2+\rho T_F,$$

$$E_2=\frac{1}{X_F}\int_0^{X_F}[Y_d(x)-Y(x)]^2dx, \qquad (6\text{—}1)$$

where X_F and T_F are the distance and the time required to a termial respectively, and T_F is in inverse proportion to the mean velocity. $Y_d(x)$ is the input function and $Y(x)$ the output of the handle system. ρ is the weighting coefficient to the time required.

When tracking M-sequence, three kinds of values; $\rho=5$, 10 and 15 were taken, and when tracking the other input functions, the value of $\rho=5$ was taken. There is no doubt that the purpose of the experiment is not to let the operator estimate the value itself of the weighting coefficient. ρ is nothing but representing the relative relation between T_F and E_2. The duration of each trial run depended on the input functions and consequently the mean velocities, but they were within 60 sec at most. After each trial, E_2, T_F and $P.I.$ were immediately computed and were put before the operator.

In case of tracking M-sequence (Y_M) and random signal (Y_D), the operator was trained to reach a stable level of performance index $P.I.$ In general, at least twenty, and often thirty, trial runs with preview length were carried out before recorded runs were made with a given preview length. After the experiments of the two inputs above were finished, the others were carried out. The subjects were three male students.

6. 3. *Experimental Results*

6. 3. 1. *The performance index and the tracking behaviors of the operator*

We at first examine if the operator grasps the meaning of the performance index Ep. (6—1). Fig. 6. 3 shows the relations between mean square value E_2 of the error and the time required T_F and the weighting coefficient ρ, where the input function is M-sequence (Y_M). The average values and the standard deviations are calculated over 15 trials (5 trials by each subject).

At every preview length, as the weighting coefficient decomes greater, the time required decreases and the mean square value increases. That is, when the weight on the time required is great, the operator pays more attention to the time required even at the sacrifice of the error. From this facts, it can be seen that after skilled the operator grasps the meaning of the performance index and changes his

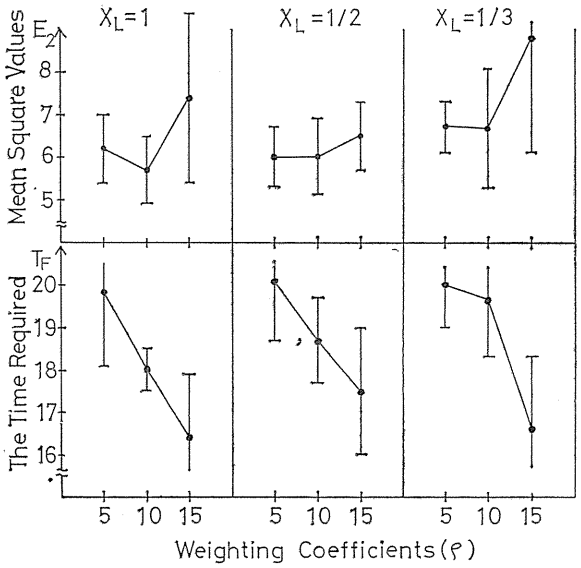

Fig. 6. 3. Mean square values and the time required (M sequence).

tracking tasks corresponding to the values of the weighting coefficient. Therefore, it has a full significance to analyze the tracking behaviors of the operator under the performance index in Eq. (6—1).

6. 3. 2. *Tracking velocity*

As shown in Fig. 6. 3, the time required (T_F) lies among 16 sec ~ 20 sec at every preview length. The full distance from start to finish of M-sequence input is 106 cm when measured on the TV screen. Then, the mean velocities are about 6. 6 cm/sec to 5. 3 cm/sec. Now the power spectral $P(\omega)$ of M-sequence is given by

$$P(\omega)=\frac{N+1}{N^2}\left(\frac{\sin\frac{\omega t_0}{2}}{\frac{\omega t_0}{2}}\right)^2 \qquad \left(0<\omega<\frac{2\pi}{t_0}\right), \qquad (6—2)$$

where N denotes the sequence period; $N=31$ in the present experiment and t_0 denotes the minimum pulse period. Since the minimum pulse width is 6 cm on the screen, the minimum pulse periods are 6/6. 6 ~ 6/5. 3 sec when the mean velocities are 6. 6 cm/sec ~ 5. 3 cm/sec. Then, the bandwidth ω_b of M-sequence are about 3. 1 rad/sec ~ 2. 5 rad/sec as calculated from Eq. (6. 2).

When, in compensatory tracking tasks, the bandwidth of the random appearing input function is 3 rad/sec and upward, the gain characteristics of the operator have a marked decline in a high frequency region, and as a natural consequence, the tracking error increases.[15] On the other hand, in the forced-paced preview tracking, the gain characteristics of the operator could be regarded as constant regardless of the preview time. Therefore, even if the operator can see ahead, the operator's gain characteristics for the input which has the bandwidth of 3 rad/sec and upward

must still have a decline in a high frequency. The time required $T_F=16$ sec in Fig. 6. 3 corresponds to $\omega_b=3.1$ rad/sec, which exceeds the critical bandwidth where

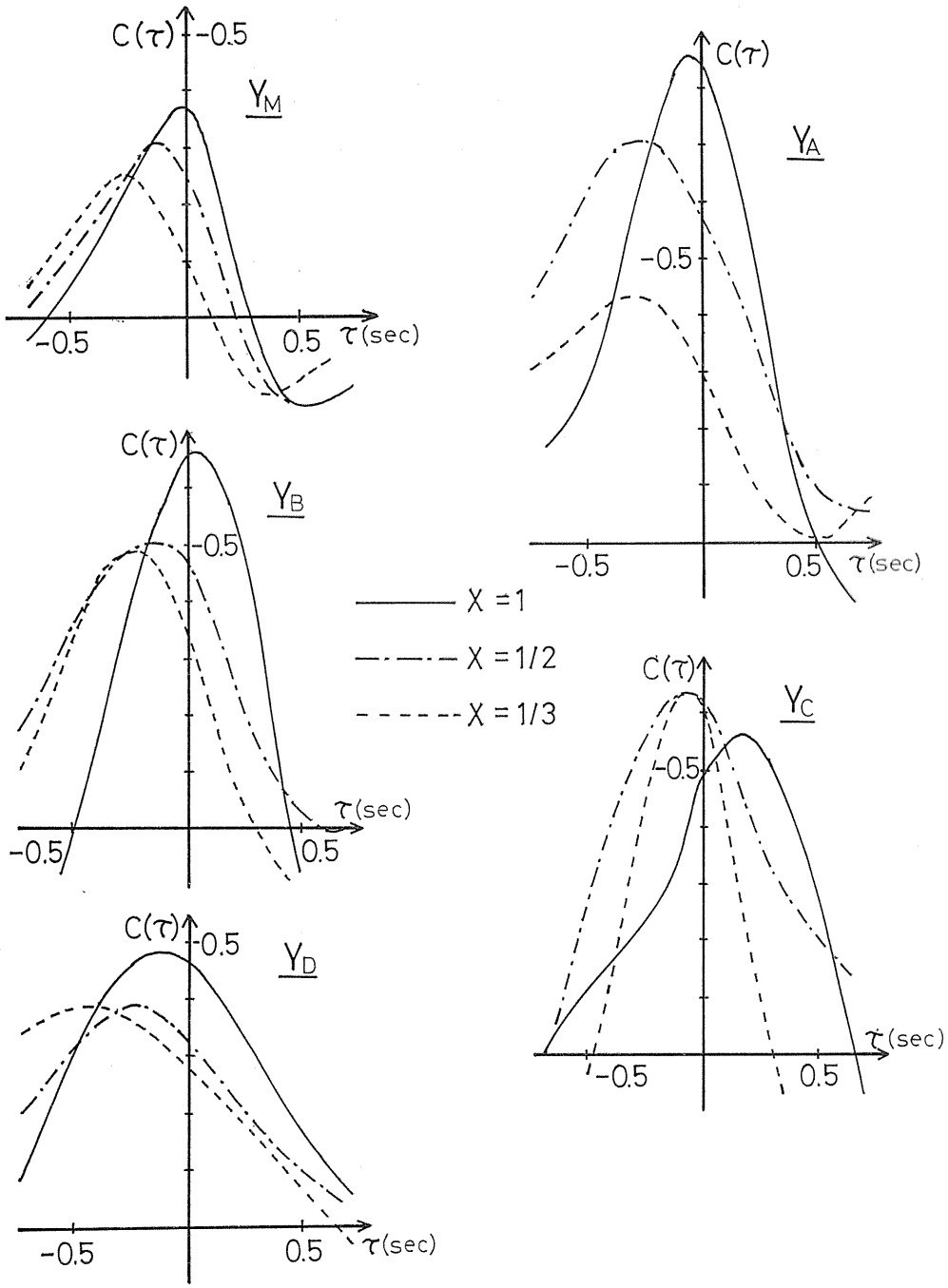

Fig. 6. 4. Cross-correlation coefficients between velocity $V(t)$ and input's time-derivative $|\dot{Y}(t)|$.

the operator is able to keep the good gain characteristics. Accordingly, it is difficult for the operator to faithfully follow the input function and as the result, the mean square value E_2 grows larger. Over against this, the time required at $\rho=5$ are 20 sec regardless of the preview length. Then, since the input bandwidth has gone down to $\omega_b=2.5$ rad/sec, the operator is able to realize the excellent tracking characteristics.

In the present experiment, since the tracking velocity is able to be changed at any moment, we should pay attention to not only the mean velocity but also the instantaneous velocity. We here discuss by what criteria the operator changes the instantaneous velocity. Fig. 6. 4 shows the cross-correlation coefficients between the tracking velocity $V(t)$ and the absolute value $|\dot{Y}(t)|$ of the input time derivative for five kinds of input functions, which are defined by

$$C(\tau)=E[V(t)-\overline{V}][|\dot{Y}(t+\tau)|-\overline{|\dot{Y}|}]/\sigma_V\cdot\sigma_{|\dot{Y}|}, \qquad (6\text{—}3)$$

where σ_V and $\sigma_{|\dot{Y}|}$ denote the standard deviations of $V(t)$ and $|\dot{Y}(t)|$ respectively, and $\overline{V}$ and $\overline{|\dot{Y}|}$ are the expected values. The every graph is obtained from the data for a subject after skilled. In either case, since they have large correlations, the input time derivative and the tracking velocity are closely connected together. And they are negative. This means that the velocity goes slow down when the input function changes largely.

When $X_L=1$, there is a peak around $\tau\cong 0$ in all input functions. This shows that the change of the velocity is synchronized in time with the change of the input function. Since there exist the delays of the controlled element and the operator himself, the operator has to control the accelerator in advance on the basis of the future input in order to synchronize the change of the velocity with that of the input. This problem will be discussed later in more detail. As the preview length becomes shorter, the peak of the correlation coefficient moves to the left gradually. This means that the operator has changes the tracking velocity late for the input's change. If the operator slows down enough at the points where the input pattern is complex, the above cannot occour. Since the performance index includes the time required T_F, however, the operator is unable to decrease the mean velocity too much. In consequence, when the preview length is limited within some extent, it is unavoidable, even in self-pacing, that the operator's response is late for the input's change.

6. 4. *Control Structures of Self-paced Preview Tracking*

We propose a self-paced preview control model as the block diagram of Fig. 6. 5. It is composed of three subblocks; (i) the first transfoms the input course as a function in space into a function in time, (ii) the second transforms the input pattern ahead into the desired input at the present time which is followed by the succeeding compensatory closed-loop system (control of handle system), (iii) the third transforms the input pattern ahead into the desired velocity at the present time which is followed by the similar closed-loop system (control of accelerator system). We discuss the mechanisms of these block diagrams in the following.

Though the input in the experiment is given as a function in space, it is natural to assume that what greets the operator's eyes is the time function transformed through the instantaneous tracking velocity. That is, the input curve $Y_d(\sigma)$;

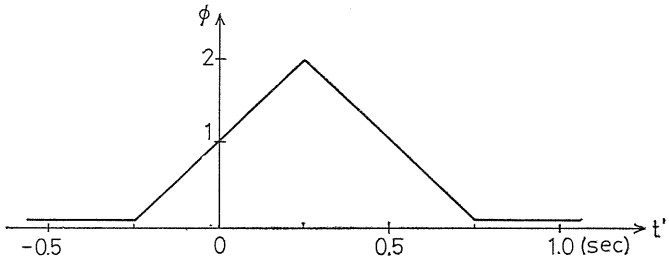

Fig. 6. 5. Self-paced preview control model.

$\sigma \in [x(t),\ x(t)+x_L]$ within the preview length at the time t is transformed into the input $Y_d(\tau)$ in time through the instantaneous velocity $V(t)$. Then the relation between σ and τ is defined by

$$\tau = t + (\sigma - x(t))/V(t), \tag{6—4}$$

where $\tau \in [t,\ t+t_f]$, $t_f = x_L/V(t)$. In the other words, $Y_d(\tau)$ is obtained when we go ahead within the preview length with keeping the preview velocity $V(t)$ constant.

Next, we have to discuss the methods which define the control signal $U_Y(t)$ of the handle system and the control signal $U_X(t)$ of the velocity control unit on the basis of the future input pattern $Y_d(\tau)$. Since the input has been already given as a time function at this step, the handle system is forced-paced preview tracking tasks. Therefore, the preview model in the preceding chapter is applicable to the handle system without any modification.

On the other hand, the desired velocity of the accelerator system is defined from the future input pattern $Y_d(\tau)$. We assume here that the operator decides the control signal $U_X(t)$ only on the basis of the future input pattern $Y_d(\tau)$. Then, the block Φ which transforms $Y_d(\tau)$ into the desired velocity $V_d(t)$ is defined by

$$m(t) = \int_{t-t_f}^{t+t_f} \phi(\tau - t)[(1-\alpha)|dY_d(\tau)| + \alpha|dDY_d(\tau)|], \tag{6—5}$$

$$\hat{V}_d(t) = V_0 \exp(-m(t)), \tag{6—6}$$

where, $DY_d(t) = \lim_{t \to +0} [Y_d(t) - Y_d(t-h)]/h$. α is the weighting coefficient and $t_f (= x_L/V(t))$ is the preview time. V_0 is the velocity when $m(t) = 0$, i. e., when the future input $Y_d(\tau)$ makes no change. Eqs. (6—5) and (6—6) are empirical equations obtained by the facts that there were negative correlations between the tracking velocity and the absolute value of the input time derivative. The second derivative is included to make possible to deal with the input such as triangular wave. In case of triangular waves, if only the first derivative is included, $m(t)$ does not change even at the apex.

Eq. (6—5) is the extended convolution integral, but the shape of the weighting function $\phi(t')$ is not yet given. We are unable to identify the shape directly from the experimental results. However, the block Φ must be able to compensate the delays of the operator himself and the velocity control unit. Therefore, we assume the shape of Fig. 6. 6 which has a peak value around $t' = 0.25$ sec similar to Fig. 5. 8.

The point is different from $Wt_f(t')$ that $\phi(t')$ weights not only the future value but also the past value of the input. Let $\phi(t')$ has a value only toward the future, then it should be noted that the stepwise variations of the input function produces

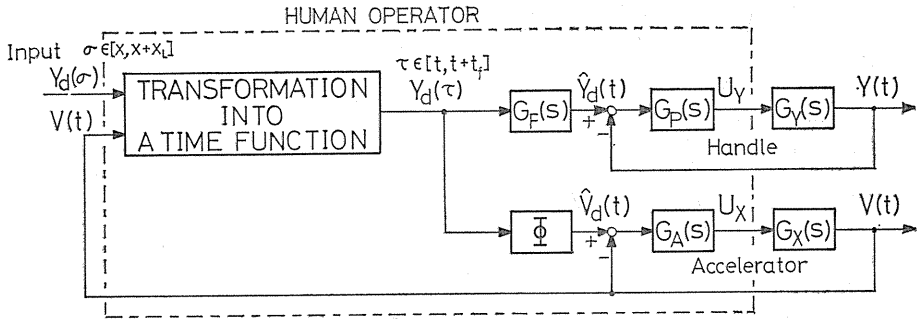

Fig. 6. 6. Weighting function $\phi(t')$ into the future and the past.

the uncontinuous desired velocity $\hat{V}_d(t)$ as seen in Eqs. (6—5) and (6—6). However, since the operator knows well the dynamic characteristics of the velocity control unit, it is not natural to assume that the operator has an uncontinuous function as the desired velocity $\hat{V}_d(t)$. Therefore, $\phi(t')$ has a value toward both the past and the future.

Considering that the operator controls the accelerator to follow its $\hat{V}_d(t)$, the closed-loop system becomes a servo system, i. e., compensatory control system. It can be approximately represented by the conventional model of the operator with unpredictable type inputs. Crossover model is adopted here again.

In the present preview control model, when the tracking velocity is slow, t_f is large, and in consequence the input pattern is prolonged on the time axis. Conversely, when it is quick, the input pattern is compressed. Since the weighting function W_{t_f} and ϕ have a peak at $t'=0.25$ sec, in the former, attention is paid to the input near the present point, while, in the latter, to the input more ahead. This coincides well with our driving sense. When the portion of large variations of the input curve comes into the preview length, the velocity begins to slow down. The nearer it comes to the point at 0.25 sec ahead, the more the velocity slows down. Thus, the input curve is transformed into a gentle slope function on the time axis, and in consequence, the operator need not to quickly manipulate the handle.

Fig. 6. 7 shows the computer simulation of the self-paced preview model and the comparison with the operator's response, where the input is random signal. Model parameters are given as $V_0=310$ (about 9 cm/sec on the screen) and $\alpha=0$, i. e., $m(t)$ is computed in terms of only the first derivative of the input function. In case of the inputs other than the random signal, only the correlation coefficients between the model's outputs and the operator's responses are shown in Table 6. 1. The correlation coefficients $C_{V\cdot V_M}$ between both the velocities lies in 0.7 to 0.9 and the ones $C_{Y\cdot Y_M}$ of the handle outputs are almost 1. The simulation results show to fit in well with the operator's response.

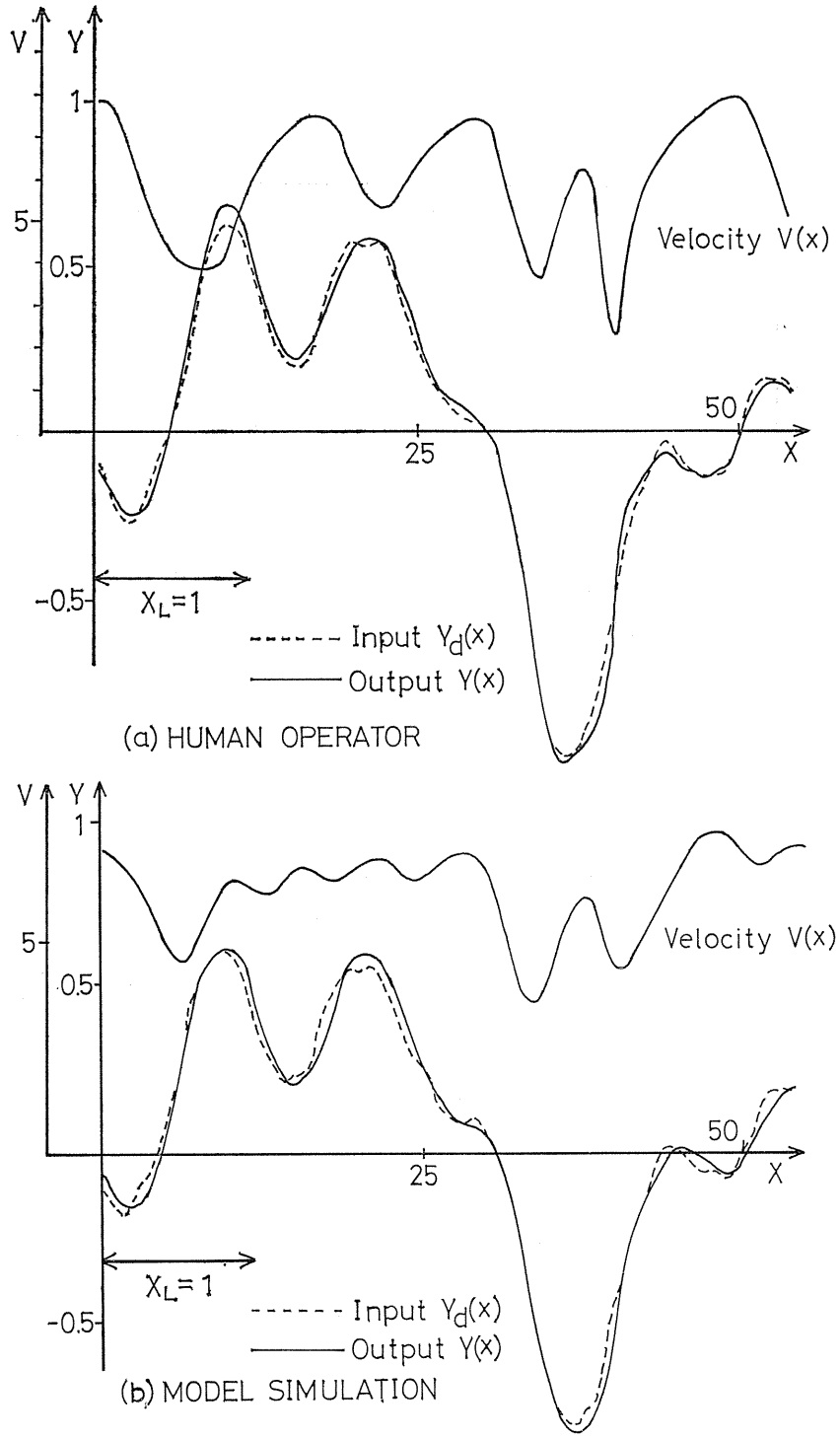

Fig. 6. 7. The computer simulation of the self-paced preview model and the comparison with a trained operator's response (random input).

Table. 6. 1. The correlation coefficients between the model's outputs and the operator's responses.

Input	$C_{Y \cdot Y_M}$	$C_{Y \cdot Y_M}$
M-sequence (Y_M)	0.88	0.98
Trapezoid (Y_A)	0.74	0.99
Semicircle (Y_B)	0.72	1.0
Triangular wave (Y_C)	0.68	1.0

6. 5. *Summary*

The following facts on self-paced preview tracking have been drawn:

(1) When the performance index includes both the error and the time required, the operator seems to decide the mean velocity such that the input bandwidth is not exceeding 3 rad/sec and the desired preview time is ensured.

(2) In addition, the instantaneous tracking velocity has large correlation with the variations of the input pattern which the operator sees at the present point.

(3) As the preview length becomes shorter, the operator tends to change the tracking velocity later for the input's change.

(4) We proposed the self-paced preview control model composed of three sub-blocks; i) the first transforms the input course as a function in space into a function in time, ii) the second transforms the input pattern ahead into the desired input at the present time, which is followed by the succeeding closed-loop system, iii) the third transforms the input pattern ahead into the desired velocity at the present time which is followed by the similar closed-loop system. The computer simulation shows to fit in well with the operator's responses. When the velocity is slow, the preview model pays attention to the input near the present, while when it is quick, to the input more ahead.

It remains, however, to consider the relation between the performance index and the mean velocity, and the mutual interference between the handle and the accelerator systems. It is also an interesting problem to extend to the three dimensional input pattern.

7. Conclusion

In the present paper, we discuss the tracking characteristics of the human operator in functional aspects. First, according to how man obtains the information about the input in the future, manual tracking systems were grouped into three classes; predictive, precognitive and preview control systems, the structures of which were analyzed from a view point of the tracking control theory. Then, when the operator sees only the instantaneous error, we experimentally investigated how the tracking bahaviors varied from precognitive control to predictive control with input signal regularity (coherence). In the chapter 4, further, we attempted to mathematically describe the precognitive tracking behaviors of the operator and

made the control structures clear. The idea of precognitive control had been proposed from early on. However, the experimental results of the control performances and the frequency characteristics etc. were paid attention to and the control structures were not refered to.

Next, we analyzed forced-paced and self-paced preview tracking tasks on the basis of both the experiments and the control theory, and the following conclusions were drawn: (1) The utilization of the future input by the operator has much effect on compensating the phase delay of himself and the controlled element. (2) The future input slightly beyond $t_f=0.5$ sec ahead is scarcely utilized. (3) The preview behavior of the human operator is not a feedfoward control. Rather, it is a feedback control with a touch of feedfoward because of his uncertainty. If the preview time is short, however, it has been found that the operator must behave as a feedfoward system to obtain the necessary phase lead. (4) In case of self-pacing, the operator decides the mean velocity such that the input bandwidth is not exceeding 3 rad/sec, and in addition, the instantaneous tracking velocity has large correlation with the variations of the input pattern which the operator can see at the present point. (5) The forced-paced preview behavior of the operator can be represented approximately by the model which consists of a series connection of the feedfoward block processing the future input and the closed-loop portion having compensatory behavior. (6) In case of self-pacing, we add the block which transforms the input course in space into a function in time and the one which transforms the future input into the present time.

In the future, it is expected to apply these results to the tracking mechanisms of robots and automatic driving cars, and synthesis of biped locomotion.

Acknowledgment

The authors gratefully acknowledges that this project was made possible through Grant in aid for scientific research, 1976 of the Ministry of Education and the contributions to this work of Mr. Watanabe S., Mr. Hayami H., Mr. Imai N., Mr. Doi T., Mr. Shimizu H. and Mr. Takeuchi A. who assisted in the experiments and in the analysis of the data.

References

(1) E. S. Krendel & D. T. McRuer: "A Servomechanisms Approach to Skill Development", J. Franklin Inst. Vol. 269, Jan. 24/42 (1960).
(2) T. B. Sheridan: "Three Models of Preview Control", IEEE Trans. on Human Factors in Electronics, Vol. HFE-7. No. 2, 91/102 (1966)
(3) D. T. McRuer, D. Graham, E. S. Krendel & W. Reisener: "Human Pilot Dynamics in Compensatory System", AFFDL-TR-65-15 (1965).
(4) J. H. Milsum: "Biological Control Systems Analysis", McGraw-Hill (1966).
(5) A. Tustin: "The Nature of the Operators Response in Manual Control and its Implications for Controller Design", J. Inst. Elect. Engr. Part II-A. 94, 190/202 (1947).
(6) L. R. Young: "On Adaptive Manual Control", IEEE Vol. MMS-10, No. 4, Part II, 292/331 (1969).

(7) M. Iguchi: "Man-Machine System", Information Science Series, B9-2, Kyoritsu Publication, (1970).
(8) R. G. Costello & T. J. Higgins: "An Inclusive Classified Bibliography Pertaining to Modeling the Human Operator as Element in an Automatic Control System", IEEE Trans. on Human Factors in Electroncis, Vol. HFE-7, No. 4, 174/181 (1966).
(9) J. E. Elkind & C. D. Forgie: "Characteristics of the Human Operator in Simple Manual Control Systems", IRE Trans. on Automatic Control, Vol. AC-4, May, 44/55 (1959).
(10) Thomas B. Sheridan & William R. Ferrell: "Man-Machine Systems: Information, Control, and Decision Models of Human Performance", The MIT Press (1974).
(11) D. T. McRuer, D. Graham & E. S. Krendel: "Manual Control of Single-Loop Systems: Part I", Jr. of Franklin Institute, Vol. 283, No. 1, 1/29 (1967).
(12) D. T. McRuer, D. H. Weir, H. R. Jex & R. E. Magdaleno: "Measurement of Driver-Vehicle Multiloop Response Properties with a Single Desturbance Input", IEEE Trans. on Systems, Man and Cybernetics, Vol. SMC-5, No. 5, 490/497 (1975).
(13) E. A. King-Smith: "Predictive Compensation in Time-Delay Manual Control Systems", NASA. Spec. Publs., 253/274 (1969).
(14) D. T. McRuer & D. H. Weir: "Theory of Manual Vehicular Control", IEEE Trans. on Man-Machine Systems, Vol. MMS-10, No. 4, Part II, 257/291 (1969).
(15) D. T. McRuer & H. R. Jex: "A Review of Ouasi-Linear Pilot Models", IEEE Trans. Human Factors in Electronics, Vol. HFE-8, No. 3, 231/249 (1967).
(16) W. H. Levison, S. Baron & D. L. Kleinman: "A Model for Human Controller Remnant", IEEE Trans. on Man-Machine Systems, Vol. 10, No. 4, 101/108 (1969).
(17) D. L. Kleinman, S. Daron & W. H. Levison: "An Optimal Control Model of Human Response Part I: Theory and Validation", Automatica, Vol. 6, 357/369 (1970).
(18) S. Baron, D. L. Kleinman & W. H. Levison: "An Optimal Control Model of Human Response Part II: Prediction of Human Performance in a Complex Task", Automatica, Vol. 6, 371/383 (1970).
(19) D. L. Kleinman & S. Baron: "A Control Theoretic Model for Piloted Approach to Landing", Automatica, Vol. 9, 339/347 (1973).
(20) R. D. Wierenga: "An Evaluation of a Pilot Model based on Kalman Filtering and Optimal Control", IEEE Trans. on Man-Machine Systems, Vol. MMS-10, No. 4, 108/117 (1969).
(21) G. A. Bekey: "The Human Operator as a Sampled-data System", IRE Trans. on Human Factors in Electronics, Vol. HFE-3, No. 2, 43/51 (1962).
(22) R. W. Pew, J. C. Duffendack & L. K. Fensch: "Sine-Wave Tracking Revisited", IEEE Trans. on Human Factors in Electronics, Vol. HFE-8, No. 2, 130/134 (1967).
(23) E. C. Poulton: "Postview and Preview in Tracking with Complex and Simple Inputs", Ergonomics, Vol. 7, No. 3, 257/266 (1964).
(24) T. B. Sheridan, W. M. Johnson, A. C. Bell & J. G. Kreifelt: "Control Models of Creatures Which Look Ahead", Proc. 5th IEEE National Symp. on Human Factors in Electroncis, May. 229/240 (1964).
(25) M. Hayase & K. Ichikawa: "Optimal Servosystem Utilizing Future Value of Desired Function", Trans. SICE (Japan), Vol. 5, No. 1, (1969).
(26) M. Tomizuka: "The Optimal Finite Preview Problem and Its Applicaiton to Man-Machine Systems", Ph. D. Dissertation, Dept. of Mech. Eng., M. I. T., Cambridge (1973).
(27) M. Ito & K. Ito: "On the Predictive, Precognitive and Preview Control Systems", Trans. Elec. Engrs. Japan, Vol. 93-C, No. 11 (1973).
(28) J. G. Truxal: "Automatic Control System Synthesis", McGraw-Hill. (1955).
(29) S. P. Bhattacharyya & J. B. Pearson: "On the Linear Servo-mechanism Problem", Int. J. Control, Vol. 12, No. 5, 795/806 (1970).
(30) S. Hosoe & M. Ito: "On Error Systems in Linear Servo Problems", Trans. Elec. Engrs. Japan, Vol. 92-C, p. 269 (1972).
(31) D. G. Luenberger: "Observing the State of a Linear System", IEEE Trans. Military Electronics, Vol. MIL-8, April, 74/80 (1964).

(32) J. B. Pearson: "Compensator Design for Dynamic Optimization", Int. J. Control, Vol. 9, No. 4, 473/482 (1969).
(33) T. Tsuchiya: "Tracking System Utilizing Predicted Value of Desired Signal", System and Control, Vol. 16, No. 1, p. 73 (1973).
(34) M. Ito: "System Control Theory", Shoko-do Publ. (1973).
(35) M. Athans & P. L. Falb: "Optimal Control". McGraw-Hill. p. 750 (1966).
(36) J. H. Wilkinson: "The Algebraic Eigenvalue Problem", Oxford Clarendon Press., 13/17 (1965).
(37) R. E. Kalman, Y. C. Ho & K. S. Narendra: "Controllability of Linear Dynamical Systems", Contributions to Differential Equ. Vol. 1, No. 2, 189/213 (1963).
(38) K. Ito & M. Ito: "Precognitive Control Behaviors of the Human Operator in Manual Control Systems", The Japanese Jr. of Ergonomics, Vol. 11, No. 4, (1975).
(39) E. C. Poulton: "Tracking Skill and Manaul Contrel", Academic Press. p. 107 (1974).
(40) K. Ito, H. Hayami & M. Ito: "A Model for Precognitive Control Behavior of Human Operator in Manual Control Systems", Trans. SICE (Japan) Vol. 9, No. 1, p. 37 (1973).
(41) K. Ito & M. Ito: "On the Tracking Behavior of the Human Operator in Preview Control Systems", Trans. Elec. Engrs. Japan, Vol. 95-C, No. 2, p. 30 (1975).